Specific Luminosity Limit of e+e- Colliding Rings

Richard Talman
Laboratory of Elementary Particle Physics, Cornell University, Ithaca, NY, USA
(Dated: 11 April, 2002)

The luminosity in flat-beam circular colliders is known to "saturate" at some "threshold" beam current above which (because the beam height grows) the luminosity varies (only) linearly with beam current, making both the "specific luminosity" (luminosity/current) and the "beam-beam tune shift parameter" ξ_y independent of current. The purpose of this paper is to calculate ξ_y analytically with the goal of maximizing the luminosity. A zero parameter application of the theory to 13 existing storage ring configurations yields theory/experiment equal to 1.26 ± 0.45 for $\xi_{y,\max.}$. Parameter values (especially tunes Q_x, Q_y, and Q_s) expected to maximize ξ_y are given. The most-favored tune combinations seem not to have been tried so far in colliding beam facilities.

The vertical beam growth is ascribed to "parametric pumping" of the vertical betatron amplitude of *each* individual particle by its own (inexorable) horizontal and longitudinal oscillation. A unique determination of the distribution of *all* particles then follows from a *saturation principle* which asserts that *the beam height adjusts itself to the smallest value for which the least stable particle (of probable amplitude) is barely stable.*

The difference equation describing the pumping can be solved by numerical iteration or, because it is (almost) linear, it can be solved analytically, at least for amplitudes small enough that resonances remain isolated. Because of the "aliasing" characteristic of accelerators, this equation exhibits an even richer spectrum of resonances than the Mathieu equation, which the present theory generalizes.

Contrary to the "lore" of the field (which motivates the intentional increase of δ_y using wigglers) the theory presented here predicts the dependence of luminosity on δ_y to be quite *weak*. This is not inconsistent with actual collider performance according to a survey by Rice[1] of colliding rings built so far.

PACS numbers: Valid PACS

I. BEAM-BEAM OBSERVATIONS FROM EXISTING E+/E- STORAGE RINGS

This paper is concerned with "saturation" of the specific luminosity, a phenomenon best understood by referring to experimental data. Luminosity data collected in 1985 by Seeman[2] for a variety of colliding rings (VEPP-2M, DCI, ADONE, SPEAR, CESR, PETRA, and PEP 3B) is shown in Fig. 1. In almost all cases "saturation" is observed—above some threshold the luminosity increases only linearly with current, and ξ_y is correspondingly constant.

This saturation phenomenon is consistent with observation (using synchrotron radiation) of beam shapes. For example, in an early observation at CESR, independent of beam current, the beams had r.m.s. width 1.4 mm and r.m.s. height not greater than 30 μm (diffraction limited) when the beams were separated; after being brought into collision the widths were sensibly unchanged but the r.m.s. beam heights were 58 μm and the beam height then increased proportionally with beam current. This causes the beam-beam tune shift parameter ξ_y to saturate and no longer increase with increasing beam current. That the horizontal profiles are unaffected corresponds to the assumption in this paper that this motion is "inexorable" and the beam height enlargement is ascribed to the "parametric pumping" of vertical oscillations by horizontal oscillations.

Luminosity behavior of LEP is described by D. Brandt et al.[3] Saturation of ξ_y is again observed. (There is a suggestion also of saturation of ξ_x in one case. This is mentioned only because, if true, it would contradict a fundamental assumptions of the present paper—that the horizontal motion is, except for modest tune shifts to be explained later, independent of beam current.) When running LEP at highest energy, 100 Gev, no saturation was observed up to the highest possible beam current. This would tend to contradict the model being presented except that the authors note that the coupling coefficent could not be reduced below $\kappa = 0.8\%$. According the present paper, saturation of ξ_y would set in already at arbitrarily small beam current in a perfect ring but this behavior is masked by any beam height σ_{y0} present due to single beam effects, especially coupling or vertical dispersion. This picture is supported by observed behavior, for example at CESR and PETRA, in which reducing the coupling reduces the threshold current at which saturation sets in.

In 1983, extrapolating empirically from existing rings to predict future behavior for LEP, Keil and Talman[4] conjectured that the damping decrement $\delta_y = 1/(2kf\tau)$ (where k is number of bunches, f is revolution frequency, and τ is damping time) would strongly influence the luminosity saturation behavior. Plotting $\xi_{y,\max}$ against δ_y for rings operating at the time (mainly PETRA and CESR) for values mainly in the range $0.5\times10^{-5} < \delta_y < 2\times10^{-5}$ a "strong" power law dependence $\xi_{\max} \sim \delta_y^{0.38}$ was found. The luminosity projection for LEP obtained by extrapolating this fit turned out to be almost a factor of two too low at lowest energy but roughly correct at higher

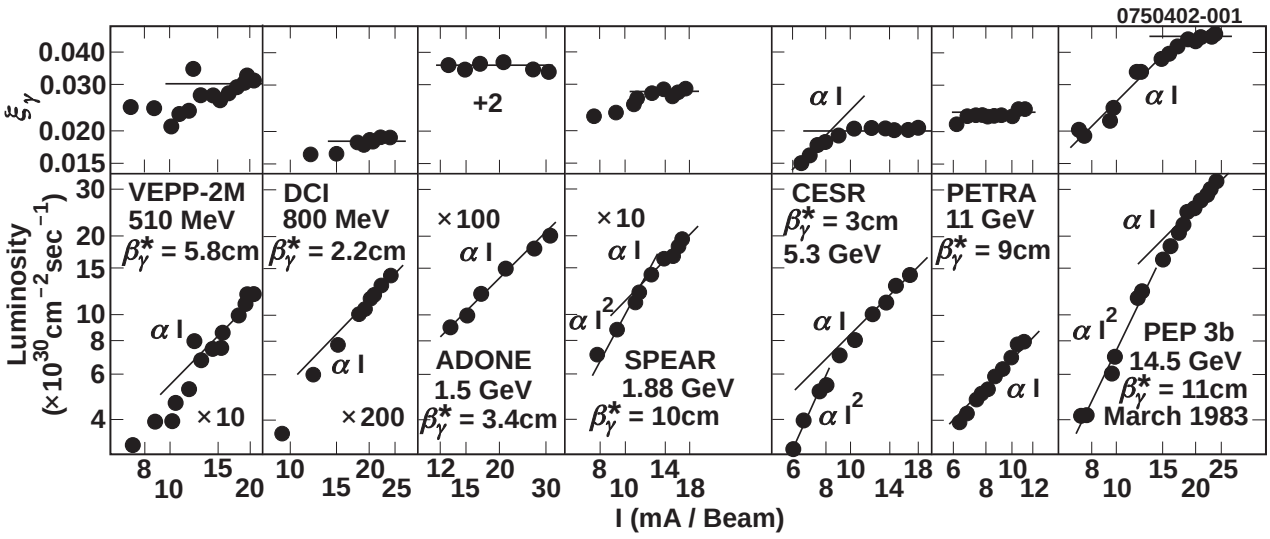

FIG. 1: Tune shift parameter "saturation" observed (pre-1985) at various e+/e- colliding beams. Copied from Seeman.[2]

energies. This suggested a power law exponent considerably smaller than 0.38. Surveying the dependence of ξ_y on δ_y, for numerous modern rings, Rice[1] has produced Fig. 2. This data shows that the power law dependence (to the extent it is applicable at all) could be as weak as $\xi_{\max} \sim \delta_y^{0.05}$.

The present paper attempts to clarify the influence of damping decrement on luminosity. The (theoretical) conclusion will be that the dependence is "weak".

II. QUALITATIVE DESCRIPTION OF THE PARAMETRIC PUMPING MODEL

It is not surprising that the (tiny) beam height is much more sensitive to the beam-beam interaction than is the (large) width. Since the horizontal motion is "hot" and the vertical "cold" any mechanism that couples these motions tends to affect the vertical motion a lot, without necessarily affecting the horizontal motion noticeably. The model proposed in this paper accepts this feature without further justification; that is, the horizontal motion of every individual electron is *inexorable*, independent of interaction with the other beam (except for a modest tune shift that allows for an increase in horizontal tune spread as the opposing beam currents are increased.)

Quite the opposite comments apply to the vertical motion. In an ideal electron storage ring, if there were no cross-plane coupling or other extraneous source of vertical excitation, ξ_y would be infinite because the vertical beam height would be zero.[10] In this ideal limit any ξ_y-dependent instability threshold whatsoever would be exceeded for any finite beam current. In particular, the resonance emphasized in this paper, parametric pumping of vertical oscillations by horizontal oscillations, is certain to occur. (The "pumped-parameter" here is the vertical betatron tune $Q_y \equiv \mu_y/(2\pi)$.) In this process, if the threshold is exceeded for any particular electron, then the vertical amplitude of this electron will increase up to a well-defined level that depends on ξ_y and on a_x, the horizontal amplitude of the particular electron. Furthermore, most of the particles must be "under the influence" of some such amplitude build up. If some large class (e.g. all particles below one half sigma horizontal amplitude) were free of perturbation, their vertical amplitudes would damp strongly, again causing unphysically large beam density.

Electrons in one beam do not interact directly with each other, but the result of their simultaneous interaction with all the particles in the other beam is a global equilibrium in which all electrons are at least marginally stable against the parametric pumping. The total effect is that the beam height will have increased to a non-zero value such that ξ_y is just low enough for this marginal stability to be achieved for (essentially) all electrons. The saturation theory (or more properly, saturation principle) now expounded is that *the beam height adjusts itself to the smallest value for which the least stable particle is barely stable.*[11] To turn this principle into a practical theoretical calculation that can predict the vertical beam height it is necessary to qualify the statement slightly by limiting it to particle amplitudes having *appreciable probability.* What is to be calculated is the saturation value of the beam-beam tune shift parameter, $\xi_{\text{sat.}}$ or equivalently, the beam height σ_y, which is proportional to $1/\xi_{\text{sat.}}$.

Single beam (noncolliding) distributions, both horizontally and vertically, are observed to be Gaussian-distributed. This is well understood as being the result of a competition between quantum fluctuations and damping, both of which are due to synchrotron radiation. It is implicit in assumptions already made that the horizontal distribution is unaffected by the beam-beam interaction.

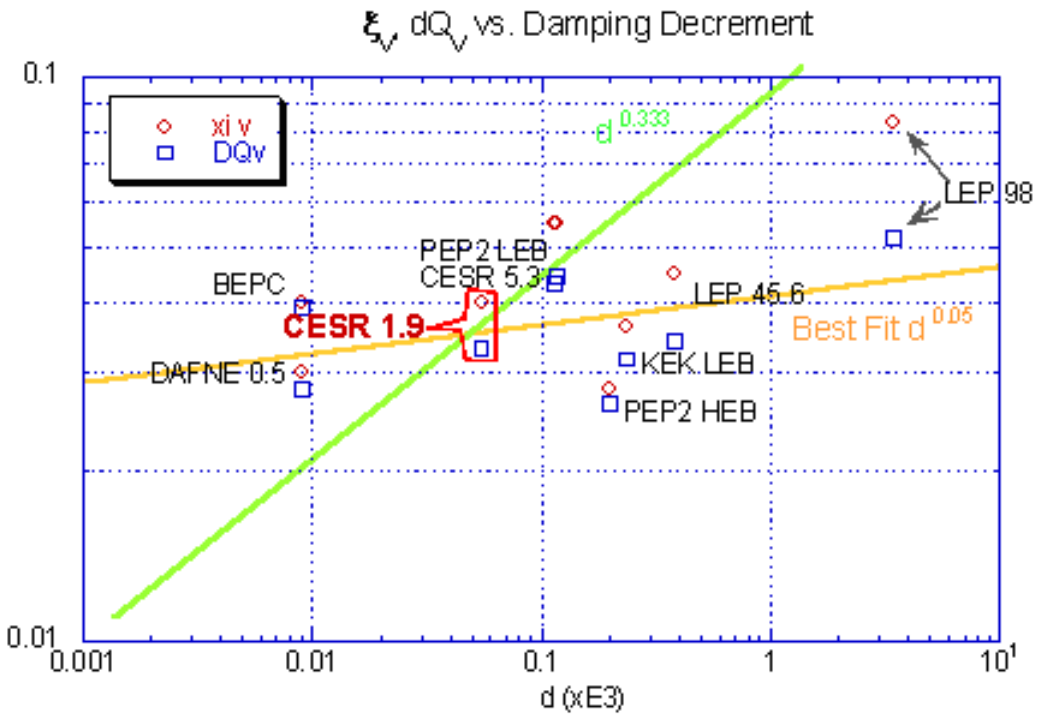

FIG. 2: Survey by Rice of the dependence of beam-beam tune shift parameter (alternate approximations are indicated ξ_v and DQv) on damping decrement δ_y (labeled as d) observed at various, not too ancient, colliding rings. Note the relatively weak dependence on δ_y.

But the parametric pumping, at a minimum, introduces a correlation between horizontal and vertical amplitudes, and is capable, therefore, of causing the vertical distribution to become non-Gaussian. An electron pumped to large vertical amplitude will tend to stay "locked" on resonance in spite of its damping, for a length of time comparable with the synchrotron radiation equilibration time (typically thousands of turns). On a longer time scale the particles will tend to be knocked off resonance by quantum fluctuation. But, because the parametric pumping mechanism is (initially) exponential, the amplitude of each particle subject to resonance grows to its limiting value within tens of turns. This paper makes no attempt to analyse the complete dynamic evolution, which is clearly very complicated. Rather it is assumed that *the equilibrium distributions remain Gaussian,* so the entire current dependence of the distribution is encapsulated in the dependence on beam current of a single parameter, σ_y.

The leading parametric resonance in mechanical oscillators occurs for drive frequency equal to twice the natural frequency; the result is a response that is a "subharmonic" of the drive. The theory of this phenomenon has a long history going back at least to Lord Rayleigh.[5] The equation of motion is known as the "Mathieu equation" or, in greater generality, the "Hill equation."[6] The leading behavior is clearly analysed by, for example, Landau and Lifshitz;[7] other than employing difference equations rather than differential equations, the present treatment mirrors their treatment. The need for difference equations arises because of the impulsive nature of the beam-beam interaction. For the same reason the phenomenon of "aliasing", without changing the essence, increases the number of possible resonances and alters the vocabulary. There are striking similarities between Mathieu domains of instability[6] and storage ring domains of instability. (See Fig. 12, which is explained in an Appendix B.) Because the bunch distributions are symmetric horizontally the vertical tune modulation occurs at tune $2Q_x$. Because of the subharmonic nature mentioned in the previous paragraph this causes resonance at $Q_y = (2Q_x)/2 = Q_x$. Even though this is the same condition as for the so-called "difference resonance" (or "coupling resonance" in accelerator physics jargon) the nature of the resonances are completely different, for example because the coupling resonance is driven by skew quadrupole forces. Furthermore parametric resonance is comparably effective for both sum and difference resonances, $Q_x \pm Q_y =$ integer.

Except for "detuning" at large vertical amplitudes the equations governing parametric pumping are linear. The detuning can be accounted for using well-established mathematical approximations, for example as described by Migulin.[8]

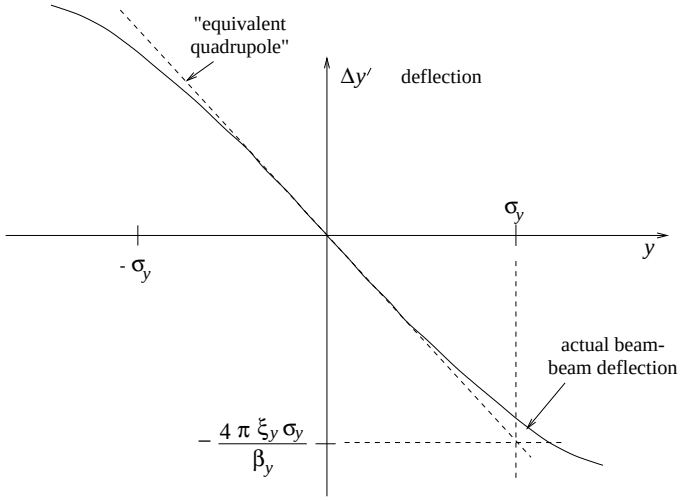

FIG. 3: Dependence of vertical deflection $\Delta y'$ on vertical displacement y. The deflection of an "equivalent" quadrupole of strength $q = -4\pi\xi/\beta$ is also shown. For an e+e- collider $\xi > 0$.

III. DIFFERENCE EQUATION FOR VERTICAL MOTION

As illustrated in Fig. 3 the vertical deflection of an electron passing through the other beam at a location with lattice function β is[12][13]

$$\Delta y' = -\frac{4\pi\xi}{\beta}\sqrt{\frac{\pi}{2}}\,\sigma\,\mathrm{erf}(\frac{y}{\sqrt{2}\,\sigma}) \approx -\frac{4\pi\xi}{\beta}\,y\,(1-\frac{y^2}{6\sigma^2}), \quad (1)$$

where the vertical distribution has been assumed to be Gaussian with r.m.s. size σ and the error function dependence results from direct application of Gauss's law assuming $\sigma << \sigma_x$. That the appropriate numerical factor has been introduced so that ξ is "beam-beam tune shift" for a small amplitude particle can be seen: a quadrupole of strength q causes deflection $\Delta y' = qy$ which causes small amplitude tune shift $\Delta Q = -\beta q/(4\pi)$.[14] The linear part of the beam-beam deflection is labeled "equivalent quadrupole" in Fig. 3.

To account for the damping that accompanies synchrotron radiation one introduces a small "damping decrement" δ, so that the once-around transfer map in "Twiss form" is

$$\begin{pmatrix} y \\ y' - \Delta y'/2 \end{pmatrix}_{t+1} = \exp(-\delta) \begin{pmatrix} C_0 + \alpha S_0 & \beta S_0 \\ -\gamma S_0 & C_0 - \alpha S_0 \end{pmatrix} \begin{pmatrix} y \\ y' + \Delta y'/2 \end{pmatrix}_{t} \quad (2)$$

and a similar equation can be written for backwards propagation from t to $t-1$. Note that y' is evaluated at the center of the other beam. I am using the notation $C_0 \equiv \cos\mu_0$ and $S_0 \equiv \sin\mu_0$. For these two maps the top equations are

$$\exp(+\delta)y_{t+1} = (C_0 + \alpha S_0)y_t + \beta S_0(y' + \Delta y'_t/2), \quad (3)$$
$$\exp(-\delta)y_{t-1} = (C_0 - \alpha S_0)y_t - \beta S_0(y' - \Delta y'_t/2). \quad (4)$$

Treating δ as small and adding these equations to eliminate y' yields[15]

$$y_{t+1} = \frac{2C_0 y_t - y_{t-1}(1-\delta) + \beta S_0 \Delta y'_t(x_t, y_t, s_t)}{1+\delta}. \quad (5)$$

This formula is extremely convenient for *numerically* evolving y into the future by simple iteration; the only substantial calculation required is the determination on each iteration of $\Delta y'_t$ (whose dependence also on on transverse coordinate x_t and longitudinal coordinate s_t will be introduced shortly.) This evolution can be *stable* or *unstable* in ways to be analysed. Once $\Delta y'_t$ has been spelled out explicitly, Eq. (5) represents the entire saturation theory—$\xi_{\mathrm{sat.}}$ is the largest value for which all amplitudes (except those negligibly far out in the "tails" of the distribution) are stable. This calculation can be performed numerically by checking the stability of Eq. (5) for a sufficiently representative selection of amplitudes and a sufficiently large number of turns.

Within the limitation of the model (for example the uncertainty in picking what constitutes a "probable amplitude" in the saturation principle) the numerical procedure just described can be arbitrarily accurate but, being numerical, it provides little intuitive guidance as to the essence of the process. For such guidance an *analytic* solution of difference Eq. (5) is useful, even if it is quantitatively inaccurate. It is convenient to set $\delta = 0$ for the moment, planning to account for damping later; to approximate the error function according to the final version of Eq. (1); and to move the linear part of the deflection to the left hand side of the equation. Then the

equation of vertical motion is

$$y_{t+1} - 2Cy_t + y_{t-1} = S\,4\pi\xi\,\frac{y^2}{6\sigma^2}\,y. \tag{6}$$

Here we have defined $C \equiv \cos(\mu_0 + 2\pi\xi)$, $S \equiv \sin(\mu_0 + 2\pi\xi)$ in order to incorporate the linear part of the beam-beam deflection into the "unperturbed motion". If the r.h.s. is evaluated for "zero'th approximation" motion $y_t = a_y \cos\mu t$, and only the "fundamental" Fourier component (varying as $\cos\mu t$) retained, the result is

$$\frac{S\pi\xi}{2}\,\frac{a_y^2}{\sigma^2}\,a_y\cos\mu t. \tag{7}$$

Resubstituting $a_y\cos\mu t = y_t$, this term can be incorporated approximately into the equation of motion by defining an amplitude-dependent coefficient,[16]

$$\bar{C} = \cos\bar{\mu} = C + \frac{S\pi\xi}{4}\,\frac{a_y^2}{\sigma^2} \approx C + \frac{S\pi\xi}{4}\,(1 - \exp(-\frac{a_y^2}{\sigma^2})). \tag{8}$$

This transforms the equation of motion into

$$y_{t+1} - 2\bar{C}y_t + y_{t-1} = \beta S\,\Delta y'_t, \tag{9}$$

where $\Delta y'_t$ is any not-yet-included perturbation. (It is not necessary to replace S by corrected value $\bar{S}$ since this factor appears only in the perturbing term.) Though $\bar{C}$ will be obtained directly from Eq. (8) when it is needed, the tune at amplitude a can be expressed directly by expanding Eq. (8);

$$\bar{\mu} = \mu_0 + 2\pi\xi\,(1 - \frac{1}{8}\,(1 - \exp(-\frac{a^2}{\sigma^2}))) \equiv \mu - \frac{\pi\xi}{4}\,(1 - \exp(-\frac{a}{\sigma^2})). \tag{10}$$

The amplitude-dependent part becomes increasingly negative as a increases, which causes the tune shift to be less positive than would be given by the linearized focusing force alone. Until amplitude-dependent detuning becomes an issue there will be no need to distinguish between $\bar{C}$ and C since instability thresholds occur for amplitudes small enough that $\bar{C} \approx C$.

The dependence of horizontal tune on horizontal amplitude will be much like that for the vertical motion. The leading variation of $\Delta x'$ is proportional to $1 - x^2/(2\sigma_x^2)$; (just as in Eq. (1).)

IV. "SUBHARMONIC" PARAMETRIC EXCITATION OF VERTICAL OSCILLATIONS

We now turn to the mathematical analysis of beam-beam distortion. From a pedagogical point of view the reader unfamiliar with difference equations might profit from first reading Appendix A, which uses difference equations to solve for betatron response to an external shaker. Because that drive is "direct" the analysis is simpler than this section requires. Higher order parametric resonances are analysed in Appendix B.

TABLE I: Fourier coefficients $B_n(a_x)$ as given by Eq. (13).

n	$Bn(0)$	$Bn(1)$	$Bn(2)$	$Bn(3)$	$Bn(4)$	$Bn(5)$
0	2.	1.58	.932	.575	.414	.326
1	0.	.196	.416	.422	.358	.299
2	0.	.0122	.0999	.199	.235	.231
3	0.	.000509	.0163	.0680	.122	.151
4	0.	.0000159	.00201	.0180	.0519	.0854
5	0.	.397e-6	.000200	.00390	.0185	.0420
6	0.	.827e-8	.0000165	.000710	.00566	.0182
7	0.	.148e-9	.118e-5	.000112	.00151	.00703
8	0.	.231e-11	.733e-7	.0000154	.000359	.00245

The vertical beam-beam deflection, given previously by Eq. (1), actually depends also on both the horizontal and longitudinal displacements. Because the beams are ribbon-shaped, and both profiles are Gaussian, the y-linearized deflection on turn t is given by[17]

$$\Delta y'_t = -\frac{4\pi\xi}{\beta}\,\exp(-\frac{a_x^2\cos^2\mu_x t}{2})\,\sqrt{1 + a_s^2\,(\frac{\sigma_s}{\beta_y^*})^2\cos^2\mu_s t}\,y_t, \tag{11}$$

where units have been chosen so $\sigma_x = 1$. ξ is now to be interpreted as the value of the tune shift parameter at $x = s = 0$. For much of this paper, in the interest of keeping the formulas simpler, I will concentrate on the transverse motion by taking $a_s = 0$. The same formulas derived for x motion can be easily transcribed to incorporate s when needed. Of course including another degree of freedom introduces many more resonances. Since $\mu_s << \mu_x$ it will be natural to regard the new resonances as "satellites" of the horizontal resonances.

It is appropriate to Fourier expand the Gaussian factor in Eq. (11);[18]

$$\Delta y'_t = -\frac{4\pi\xi}{\beta_y}\,(\sum_{n=0}^{\infty}\,(\frac{B_0}{2} + B_n\cos(2n\mu_x t)))\,y_t. \tag{12}$$

The coefficients B_n can be evaluated in terms of (modified) Bessel functions I_n using an integral from Watson, *Bessel Functions,* 6.22(4); the result is

$$B_n = 2\exp(-\frac{a_x^2}{4})\,I_n(-\frac{a_x^2}{4}). \tag{13}$$

Values of B_n are given in Table I. The first row and first column are shown only for completeness. B_0 can (and will) be set to zero as far as the mechanism of this paper is concerned. (This is consistent with the formulation described previously, where the leading effect of the beam-beam interaction was defined to be part of the unperturbed motion.) As stated earlier, because the "effective tune" of the vertical gradient acting on the particle under study is $2\mu_x$, the leading "subharmonic" resonance occurs for $\mu_x \approx \mu$.

We hypothesize the response of an individual electron to the parametric drive to be betatron motion for which

the dominant part is sinusoidal, with a frequency $\tilde{\mu}$ to be determined;

$$y_t = a\,\cos((\mu+\varepsilon_n)t)+b\,\sin((\mu+\varepsilon_n)t) \equiv a\,\cos\tilde{\mu}t+b\,\sin\tilde{\mu}t. \tag{14}$$

Here ε_n, to be defined shortly, is a "small" frequency deviation from the natural frequency. It is possible for any of the terms in the sum (12) to "resonate with" (and hence cause) this motion. The quantity $\mu+\varepsilon_n$ has been replaced by $\tilde{\mu}$ in Eq. (14) and from here on, even though this suppresses the (essential) index n. The coefficients a and b are "variation of constants" coefficients whose variation will be arranged shortly to satisfy the equation of motion. They are assumed to vary slowly with t; that is, their fractional changes per revolution are small compared to 1. If they are treated as depending on a continuous variable t, then

$$a_{t\pm1} \approx a_t \pm \dot{a}_t, \text{ and } b_{t\pm1} \approx b_t \pm \dot{b}_t. \tag{15}$$

From here on the t-subscripts on a and b will be supressed.

Combining Eq. (12) (with constant term dropped) and Eq. (14) yields

$$\begin{aligned}
\frac{-\Delta y'_t}{4\pi\xi/\beta} &= \sum_{n=1}^{\infty} B_n\cos(2n\mu_x t)\,(a\,\cos(\tilde{\mu}t)+b\,\sin(\tilde{\mu}t)) \\
&= \sum_{n=1}^{\infty} \frac{B_n}{2}\,(a\cos((2n\mu_x-\mu-\varepsilon_n^{(-)})t)-b\sin((2n\mu_x-\mu-\varepsilon_n^{(-)})t)) \\
&+ \sum_{n=1}^{\infty} \frac{B_n}{2}\,(a\cos((2n\mu_x+\mu+\varepsilon_n^{(+)})t)+b\sin((2n\mu_x+\mu+\varepsilon_n^{(+)})t)).
\end{aligned} \tag{16}$$

Any term in these sums can potentially cause resonance. The frequency offsets $\varepsilon_n^{(\pm)}$ quantify "phase offsets from nearest resonances" by the following relations (for which the overall signs are not significant)

$$\begin{aligned}
2n\mu_x+\mu+\varepsilon_n^{(+)} &= -(\mu+\varepsilon_n^{(+)}),\text{ or } \varepsilon_n^{(+)} = n\mu_x+\mu\ , \\
2n\mu_x-\mu-\varepsilon_n^{(-)} &= +(\mu+\varepsilon_n^{(-)}),\text{ or } \varepsilon_n^{(-)} = n\mu_x-\mu\ .
\end{aligned} \tag{17}$$

Presumably a particular one of these possibilities, say n,– will dominate over all others. From here on the index n will be specialized to indicate this particular dominant case. Then, dropping all other terms Eq. (16) becomes

$$\Delta y'_t = -\frac{4\pi\xi}{\beta}\,\frac{B_n}{2}\,(a\cos(\tilde{\mu}t)-b\sin(\tilde{\mu}t)). \tag{18}$$

Substitution into Eq. (9) yields

$$y_{t+1}-2\bar{C}y_t+y_{t-1} = -S\,2\pi\xi\,B_n\,(a\cos(\tilde{\mu}t)-b\sin(\tilde{\mu}t)). \tag{19}$$

(As mentioned earlier it is initially unnecessary to distinguish between $\bar{C}$ and C.) Including the time variation of a and b, Eq. (14) yields

$$\begin{aligned}
y_{t+1} = &\quad (a+\dot{a})(\cos\tilde{\mu}\cos(\tilde{\mu}t)-\sin\tilde{\mu}\sin(\tilde{\mu}t)) \\
&+ (b+\dot{b})(\sin\tilde{\mu}\cos(\tilde{\mu}t)+\cos\tilde{\mu}\sin(\tilde{\mu}t)) \\
y_{t-1} = &\quad (a-\dot{a})(\cos\tilde{\mu}\cos(\tilde{\mu}t)+\sin\tilde{\mu}\sin(\tilde{\mu}t)) \\
&+ (b-\dot{b})(-\sin\tilde{\mu}\cos(\tilde{\mu}t)+\cos\tilde{\mu}\sin(\tilde{\mu}t)).
\end{aligned} \tag{20}$$

Substituting into Eq. (19), and requiring the sine and cosine term coefficients to vanish separately yields the equations

$$\begin{aligned}
-\dot{a}\sin\tilde{\mu}+b\cos\tilde{\mu}-\bar{C}b-S\,\pi\xi\,B_n\,b &= 0 \\
\dot{b}\sin\tilde{\mu}+a\cos\tilde{\mu}-\bar{C}a+S\,\pi\xi\,B_n\,a &= 0.
\end{aligned} \tag{21}$$

Seeking a solution for which a and b exhibit time dependence of the form $\exp(i\omega t)$ yields

$$\begin{pmatrix} -i\omega & \frac{\cos\tilde{\mu}-\bar{C}-S\,\pi\xi\,B_n}{\sin\tilde{\mu}} \\ \frac{-\cos\tilde{\mu}+\bar{C}-S\,\pi\xi\,B_n}{\sin\tilde{\mu}}\,a & -i\omega \end{pmatrix}\begin{pmatrix} a \\ b \end{pmatrix} = 0. \tag{22}$$

The requirement for nontrivial solution to exist is that the determinant formed from the coefficients must vanish; this yields

$$\omega^2 = \frac{(\cos\tilde{\mu}-\bar{C})^2-(S\,\pi\xi\,B_n)^2}{\sin^2\tilde{\mu}}. \tag{23}$$

In this form the condition for *stable* motion is that ω^2 be *positive* (since the alternative yields one exponentially-growing solution.) Making the assumptions $\varepsilon_n << 1$ and $C=\bar{C}$ allows the approximations $\cos\tilde{\mu}-\bar{C}\approx -S\varepsilon$, $\sin\tilde{\mu}\approx S$. Then setting $\omega=0$ to determine the edges of a "stop band" yields[19]

$$\varepsilon^2 = (\pi\xi\,B_n)^2, \quad \text{or} \quad -\pi\xi\,B_n < \varepsilon < \pi\xi\,B_n. \tag{24}$$

By setting δ to zero we have so far been neglecting damping and have found that, even with no damping, if ε lies outside the stop band, the motion will be stable. In fact there *is* damping, as represented by $\delta \neq 0$. The threshold of instability is therefore determined by

requiring the growth rate given by Eq. (23) to be equal to δ;

$$\sqrt{-\varepsilon^2 + \pi^2\xi^2\, B_n^2} = \delta. \tag{25}$$

The band of instability is therefore given by

$$-\varepsilon_l < \varepsilon < \varepsilon_l, \quad \text{where} \quad \varepsilon_l = \sqrt{\pi^2\xi^2\, B_n^2 - \delta^2}. \tag{26}$$

For $\delta > \pi\xi B_n$ there is no unstable band at all. It is probably in this resonance-suppressing role that δ has its greatest potential influence on luminosity.

The prediction so far is that the motion is either stable or that, within a limited band, the amplitude grows exponentially without limit. Such growth would eventually invalidate the small amplitude assumption on which the equation is based and, in fact, the amplitude-dependent detuning analysed earlier limits the growth. Because of the nonlinearity, as well as the state of equilibrium with $a_y^2 = 0$ there is a state of equilibrium with $a_y^2 = a^2 + b^2 \neq 0$. Substituting for $\bar{C}$ from Eq. (8), Eq. (23) with $\omega^2 = -\delta^2$ depends on the amplitude parameter a_y. After rearrangement the condition becomes

$$\begin{aligned} \varepsilon = \; & \pm\sqrt{\pi^2\, B_n^2\, \xi^2 - \delta^2} - \tfrac{\pi\xi}{4}\,(1 - \exp(-\tfrac{a^2+b^2}{\sigma^2})) \\ \approx \; & \pm\sqrt{\pi^2\, B_n^2\, \xi^2 - \delta^2} - \tfrac{\pi\xi}{4}\,\tfrac{a_y^2}{\sigma^2}. \end{aligned} \tag{27}$$

If there is an unstable band then $\pi^2\, B_n^2\, \xi^2 - \delta^2$ is positive so picking the positive-sign square root yields a positive value for a^2 throughout the stop band of Eq. (26). This equation sets the amplitude at which the growth of vertical amplitude is limited by the amplitude-dependent detuning. The vertical amplitude of any particle whose tunes place it in the range Eq. (26) will be pumped immediately to the value given by Eq. (27). The functions of Eq. (27) are plotted schematically in Fig. 4. It can be seen that stable motion with $a \neq 0$ is even possible for $\varepsilon < -\varepsilon_l$. This asymmetry in ε will be important in interpreting numerical solutions of the master difference equation. In particular it seems to account for the numerically-observed superiority of values Q_x just above resonance compared to values just below.

For the special case $\delta = 0$ the band limits are at $\varepsilon = \pm\pi\xi B_n$ so the amplitude lies in the range $0 < a_y <\sim 2\sqrt{2B_n}\sigma$. From Table I one notes that values of B_n likely to be important vary over the range from, say, 0.05 to 0.5, depending on a_x, so the limiting amplitude ranges from close to zero up to about $2\,\sigma$. As the particle oscillates its loss of vertical amplitude due to radiation damping will tend to be replenished immediately by the pumping mechanism and the particle will oscillate rather stably for many turns. But the particle's random walk in horizontal phase space will eventually disrupt the resonance. Positive damping ($\delta > 0$) reduces the limiting amplitude (though typically very little) and, as noted previously, reduces the stop band width.

There is a certain self-consistency here—whatever the beam height is, at least approximately, the pumping mechanism provides the support for just that beam height. This "natural" relationship provides corroborates the identification of detuning as the amplitude-establishing mechanism since the height scale on which detuning occurs is about the same as the beam height itself. Just what this height σ *is* remains to be determined. The further relation that, in principle, fixes σ is that ξ depends inversely on σ. The relation can be written as

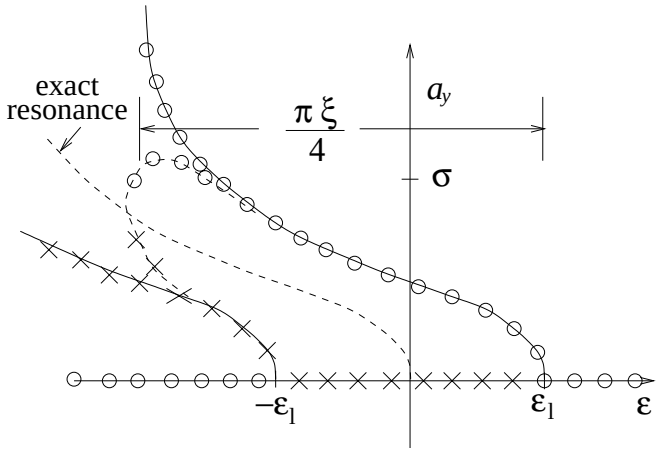

FIG. 4: Plot of Eq. (27). Open circles mark stable motion; a temporary excursion to *larger* a_y moves the system *away* from "exact" resonance which tends to *reduce* a_y. Crosses mark unstable motion. The broken curve indicates the sort of dependence to be expected from a more detailed theory including other nonlinearity.

$$\xi = \frac{I'}{\sigma}. \tag{28}$$

where I' is the beam current, as measured in units picked to make the constant of proportionality be 1. The factors entering this relation are all well known in practice.

Though it is still too encumbered with limitations to give an accurate picture, and it is not clear what form of averaging is appropriate, Eq. (27) can be manipulated to express this self-consistency semi-quantitatively. Since the beam height is supposed to be ascribable to the pumping mechanism that the equation describes, one has to suppose $a \approx \sigma$ is typical. With this assumption Eq. (27) determines ξ according to

$$\frac{1}{2}\,\xi^2 - \frac{\varepsilon}{4\pi B_n^2}\,\xi - \frac{\varepsilon^2 + \delta^2}{2\pi^2 B_n^2} \approx 0, \quad \text{assuming} \quad 16B_n^2 >> 1, \tag{29}$$

which can be solved to give

$$\xi_{\max.} \approx \frac{1}{\sqrt{2}\pi B_n}\,(\frac{\varepsilon}{2\sqrt{2}B_n} + \sqrt{\varepsilon^2 + \delta^2}). \tag{30}$$

Then σ is determined by Eq. (28). To be valid at all this formula assumes that a known resonance is dominant and that ε corresponds to that resonance. The structure of this formula predicts that the dependence of $\xi_{\max.}$ on δ is

more complicated than the power law dependence mentioned earlier. In any case the main purpose of Eq. (30) is to illustrate an "in-principle", parameter-free, determination of the limiting tune shift parameter. Since $\delta << \epsilon$ is typical, Eq. (30) exhibits only a very weak dependence on δ. This contrasts with the threshold tune shift value which, according to Eq. (48), depends sensitively on δ.

V. OTHER RESONANCES

Eq. (14) was not the most general possibility for parametric resonance. For example, suppressing the t subscripts (as before) to free up a position for Fourier indices, let us seek a solution of the form

$$y = a_0 + \sum_{m=1}^{3} a_m \cos(m\tilde{\mu}_y t) + \sum_{m=1}^{3} b_m \sin(m\tilde{\mu}_y t), \quad (31)$$

truncated, at least for the time being, at $m = 3$. Extra terms appear in Eq. (16). Suppressing the summation over n,

$$\frac{-\Delta y'_t}{4\pi\xi_y/\beta_y}\frac{2}{B_n} = 2a_0\cos(2n\mu_x t) + \sum_{m=1}^{3} a_m \cos(2n\mu_x - m\tilde{\mu}_y t) + \sum_{m=1}^{3} a_m \cos(2n\mu_x + m\tilde{\mu}_y t) - \sum_{m=1}^{3} b_m \sin(2n\mu_x - m\tilde{\mu}_y t) + \sum_{m=1}^{3} b_m \sin(2n\mu_x + m\tilde{\mu}_y t). \quad (32)$$

These lead to definitions, like those in Eq. (17), that pick out tune combinations for which the perturbed frequency matches the fundamental frequency. Recalling that $\mu_y + \varepsilon_n \equiv \tilde{\mu}_y$,

$$2n\mu_x - (s+1)\tilde{\mu}_y = \tilde{\mu}_y, \quad \text{or} \quad 2n\mu_x = (2+s)\tilde{\mu}_y, \quad (33)$$

where s is another integer. This is not the only possibility and the notation no longer identifies the particular offset ε_n that is being defined. Then Eq. (32) becomes

$$\begin{aligned}\tfrac{-\Delta y'_t}{4\pi\xi_y/\beta_y}\tfrac{2}{B_n} &= 2a_0\cos(s+2)\tilde{\mu}_y t \\ &+a_1\cos(s+1)\tilde{\mu}_y t + a_2\cos(s+0)\tilde{\mu}_y t + a_3\cos(s-1)\tilde{\mu}_y t \\ &+a_1\cos(s+3)\tilde{\mu}_y t + a_2\cos(s+4)\tilde{\mu}_y t + a_3\cos(s+5)\tilde{\mu}_y t \\ &-b_1\sin(s+1)\tilde{\mu}_y t - b_2\sin(s+0)\tilde{\mu}_y t - b_3\sin(s-1)\tilde{\mu}_y t \\ &+b_1\sin(s+3)\tilde{\mu}_y t + b_2\sin(s+4)\tilde{\mu}_y t + b_3\sin(s+5)\tilde{\mu}_y t. \end{aligned} \quad (34)$$

The case $s = 0$ was previously called "lowest order". Let us try $s = -1$, so $2n\mu_x = \tilde{\mu}_y$, or $\varepsilon_n = 2n\mu_x - \mu_y$;

$$\begin{aligned}\tfrac{-\Delta y'_t}{4\pi\xi_y/\beta_y}\tfrac{2}{B_n} &= a_1 + (2a_0 + a_2)\cos(\tilde{\mu}_y t) + \\ &+(a_1 + a_3)\cos(2\tilde{\mu}_y t) + b_2\sin(\tilde{\mu}_y t) + b_1\sin(2\tilde{\mu}_y t) \end{aligned} \quad (35)$$

where higher terms have been dropped. Eqs. (20) now acquire extra terms and Eqs. (21) generalize to multiple equations;

$$\begin{aligned} a_0 - C_y a_0 + S_y\,\pi\xi_y\,B_n\,(a_1) &= 0, \\ -\dot{a}_1\sin\tilde{\mu}_y + b_1\cos\tilde{\mu}_y - C_y b_1 + S_y\,\pi\xi_y\,B_n\,(b_2) &= 0, \\ \dot{b}_1\sin\tilde{\mu}_y + a_1\cos\tilde{\mu}_y - C_y a_1 + S_y\,\pi\xi_y\,B_n\,(2a_0 + a_2) &= 0, \\ -\dot{a}_2\sin 2\tilde{\mu}_y + b_2\cos 2\tilde{\mu}_y - C_y b_2 + S_y\,\pi\xi_y\,B_n\,(b_1) &= 0, \\ \dot{b}_2\sin 2\tilde{\mu}_y + a_2\cos 2\tilde{\mu}_y - C_y a_2 + S_y\,\pi\xi_y\,B_n\,(a_1) &= 0 \end{aligned} \quad (36)$$

From the first equation we obtain

$$a_0 = -\frac{S_y\,\pi\xi_y\,B_n}{1 - C_y}\,a_1. \quad (37)$$

As mentioned in an earlier footnote, at the stability limits the derivative terms vanish. Using this and $\cos\tilde{\mu}_y \approx C_y - S_y\varepsilon_n$ and $\cos 2\tilde{\mu}_y \approx \cos 2\mu_y$ these equations become

$$\begin{aligned} b_1\varepsilon_n &= -\pi\xi_y\,B_n\,b_2, \\ a_1\varepsilon_n &= -\pi\xi_y\,B_n\,(2a_0 + a_2), \\ b_2(C_y - \cos 2\tilde{\mu}_y) &= S_y\,\pi\xi_y\,B_n\,b_1, \\ -a_2(C_y - \cos 2\tilde{\mu}_y) &= -S_y\,\pi\xi_y\,B_n\,a_1, \end{aligned} \quad (38)$$

which yield

$$a_2 = \frac{S_y\pi\xi_y B_n}{C_y - \cos 2\tilde{\mu}_y}\,a_1, \quad b_2 = \frac{S_y\pi\xi_y B_n}{C_y - \cos 2\tilde{\mu}_y}\,b_1. \quad (39)$$

The stability limits are unbalanced;

$$\begin{aligned} \varepsilon_{n1} &= \tfrac{-S_y(\pi\xi_y B_n)^2}{C_y - \cos 2\tilde{\mu}_y}, \\ \varepsilon_{n2} &= S_y(\pi\xi_y B_n)^2\left(\tfrac{2}{1-C_y} + \tfrac{1}{C_y - \cos 2\tilde{\mu}_y}\right). \end{aligned} \quad (40)$$

This "higher order" resonance, with $n = 1, s = -1$, requires the same relation between Q_x and Q_y as the "lowest order" resonance with $n = 2, s = 0$, but the numerical factor and resonant denominators are different. Compared to the limit given in Eq. (24) these acquire factors of order $\pi\xi_y B_n$. Referring to values of B_n given in Table I, and expecting the factor $\pi\xi_y$ to not exceed, say, 0.3, the only values of n likely to be significant will not exceed a few unless one of the denominators is anomalously small. Several parametric resonances are therefore

TABLE II: The leading linear parametric resonances, including aliases. These resonance lines are plotted in Figure ??.

n	s	$\frac{2n}{2+s}\,Q_x$	aliases	$-\frac{2n}{2+s}\,Q_x$	aliases
n	s	$\frac{2n}{2+s}\,Q_x$	aliases	$-\frac{2n}{2+s}\,Q_x$	aliases
1	0	Q_x	+.5, +0, -.5	$-Q_x$	+1.5, +1, +1.5
2	0	$2Q_x$	+.5, +0, -.5, -1, -1.5	$-2Q_x$	+2.5, +2, +1.5, +1, +.5
1	-1	$2Q_x$	+.5, +0, -.5, -1, -1.5	$-2Q_x$	+2.5, +2, +1.5, +1, +.5
1	1	$2Q_x/3$	suppressed (Figure 12)	$-2Q_x/3$	suppressed

candidates to dominate the growth of the vertical beam size, even without including longitudinal oscillations.

To incorporate damping decrement δ_y one should first solve the determinant equation for the growth rate. This should then be set equal to the δ_y to find the stability limits in the presence of damping, as in Eq. (25). Simpler is to mimic Eq. (26) by interpreting ε_{n1}^2 as the square of a real frequency shift and to equate it to δ_y^2 which is the (negative) square of an imaginary frequency shift. (Doing the same with ε_{n2}^2 will not yield quite the same value. This reflects the fact that the threshold of instability need not occur at exactly $\epsilon = 0$.) The first estimate yields

$$\xi_y = \frac{\delta_y^{1/2}}{\pi B_n}\sqrt{\frac{C_y - \cos 2\tilde{\mu}_y}{\sin\tilde{\mu}_y}}. \tag{41}$$

For $s = 1$ the resonant tune relation is $2n\mu_x = 3(\mu_y + \varepsilon_n)$ or $\varepsilon_n = (2/3)n\mu_x - \mu_y$.

$$\begin{aligned}\tfrac{-\Delta y_i'}{4\pi\xi_y/\beta_y}\,\tfrac{2}{B_n} &= 2a_0\cos(3\tilde{\mu}_y t) + a_1\cos(2\tilde{\mu}_y t) + \\ &+a_2\cos(\tilde{\mu}_y t) + a_3 - b_1\,\sin(2\tilde{\mu}_y t) - b_2\,\sin(\tilde{\mu}_y t).\end{aligned} \tag{42}$$

The analogs of Eqs. (36 are

$$\begin{aligned}-\dot{a}_1\sin\tilde{\mu}_y + b_1(\cos\tilde{\mu}_y - C_y) + S_y\,\pi\xi_y\,B_n\,(-b_2) &= 0,\\ \dot{b}_1\sin\tilde{\mu}_y + a_1(\cos\tilde{\mu}_y - C_y) + S_y\,\pi\xi_y\,B_n\,(a_2) &= 0,\\ -\dot{a}_2\sin 2\tilde{\mu}_y + b_2\cos 2\tilde{\mu}_y - C_y b_2 + S_y\,\pi\xi_y\,B_n\,(-b_1) &= 0,\\ \dot{b}_2\sin 2\tilde{\mu}_y + a_2\cos 2\tilde{\mu}_y - C_y a_2 + S_y\,\pi\xi_y\,B_n\,(a_1) &= 0\end{aligned} \tag{43}$$

which yield

$$\begin{aligned}\varepsilon_n &= -\pi\xi_y\,B_n\,\tfrac{a_2}{a_1},\\ a_2(\cos 2\tilde{\mu}_y - C_y) &= -S_y\,\pi\xi_y\,B_n\,a_1,\\ \varepsilon_n &= \pi\xi_y\,B_n\,\tfrac{b_2}{b_1},\\ b_2(\cos 2\tilde{\mu}_y - C_y) &= S_y\,\pi\xi_y\,B_n\,b_1.\end{aligned} \tag{44}$$

As usual the resonances can be identified with straight lines in a resonance diagram such as Figure 5. The aliasing can be implemented using "periodic boundary conditions". When a line terminates on an integer boundary another line with the same slope starts from the same location on the opposite boundary.

Both limits are given by

$$\varepsilon_n = S_y(\pi\xi_y B_n)^2\left(\frac{1}{\cos 2\tilde{\mu}_y - C_y}\right). \tag{45}$$

The implication of equality of these limits is presumably that the stopband width is of higher order in ξ than has been used in the calculation. This probably makes this resonance unimportant and accounts for the absence of $s = 1$ stop band in Figure 12.

It is tedious to extend this calculation to higher order. In Appendix B this extension is made more systematic by using complex exponentials.

VI. IMPORTANT RESONANCES AND FAVORED REGIONS

The master formula governing exact resonance is Eq. (B7). Expressed in terms of tunes it is

$$Q = \pm\frac{2n}{2+s}\,Q_x, \tag{46}$$

where n is a positive integer and s is any integer except -2. The aliasing is such that multiples of 1/2 can be added (or subtracted) from either Q_x or Q. The leading possibilities are tabulated in Table II.

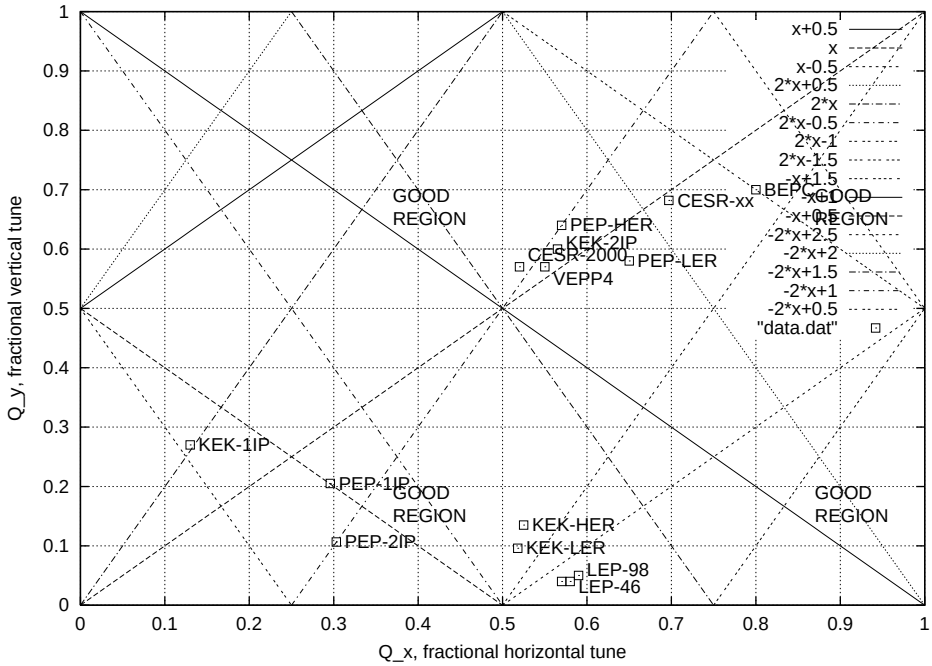

FIG. 5: Linear parametric beam-beam resonances from Table II. In all cases tunes are tune advances per IP. None of the operating points are even close to regions labeled "GOOD REGION" on the basis of the *saturation principle*, numerically investigated.

The essential feature of the parametric growth mechanism that has been analysed is that there is stability up to a threshold above which the amplitude grows rapidly to an amplitude limited by detuning. To avoid resonance the tune ranges to be avoided have to be expanded by the range of horizontal tunes. There is also a spread of vertical tunes but this mainly leads to detuning that has to be modeled explicitly, as has been discussed; this effect is automatically included in the numerical investigation described in the next section.

The single resonance model assumes that it is impossible to avoid all resonances and that, for any given operating conditions, it is necessary only to identify and analyse the dominant resonance. In this case the onset of beam growth is controlled by δ. For the lowest order ($s = 0$) resonance, according to Eq. (26), the instability sets in at

$$\xi_{n,0} = \frac{\delta}{\pi B_n}, \tag{47}$$

where the second subscript stands for $s = 0$. This is a special case of formulas for $\xi_{\rm sat.}$ derived in Appendix B which take the form

$$\xi_{n,s} = \frac{1}{\pi B_n}\,\delta^{1/(1+|s|)}\,T_{n,s}^{1/(1+|s|)}, \tag{48}$$

where $T_{n,s}$ is a trigonometric function of the tunes, whose value is approximately 1. For example, from Eq. (B19)

$$\xi_{n,-1} = \frac{\delta^{1/2}}{\pi B_n}\sqrt{\frac{C_y - \cos 2\tilde{\mu}}{S_y}}. \tag{49}$$

For this resonance the power law exponent is 0.5.

Tune combinations for which $s = 0$ yield such small values of $\xi_{y,\rm thr.}$ it seems reasonable to suppose they have always been, and will always be, avoided operationally. One might say therefore that for "unfavorable" tunes the power law exponent is ~ 1 since $\xi_{y,\rm thr.} \sim \delta_y$ For "once-removed" resonances, $s = \pm 1$, $\xi_{y,\rm thr.} \sim \sqrt{\delta_y}$ and the power law exponent is 0.5.

The single resonance model may give a good description in regions where a single resonance is dominant, but in these regions the saturation threshold is necessarily very low. Such regions are avoided in practice since the goal of colliding beams is high luminosity and there is too much operational overhead to spend machine studies time investigating unpromising tune combinations. As a result there tends to be little data with which to test the single resonance model. In practice the tunes are adjusted to be roughly equidistant from the two or three nearest resonances, invalidating the single-resonance assumption. The numerical approach, to be descibed next, automatically includes the effects of overlapping resonances.

VII. SOLUTION OF THE DIFFERENCE EQUATION BY NUMERICAL ITERATION

The analytic solution given so far breaks down when the particle amplitude increases to a value such that more than one resonance is significant. Then a numerical approach is required. The difference equation (5) and deflection formula (1) can be combined into a formula that makes turn-by-turn iteration easy;

$$y_{t+1} = \frac{1}{1+\delta}\left(2C_0 y_t - y_{t-1}(1-\delta) - 4\pi\xi S_0 \times \exp(-\frac{a_x^2\cos^2(\mu_x(a_x)(t+t_x))}{2})\sqrt{1+(\frac{\sigma_s}{\beta_y^*})^2\, a_s^2\,\cos^2(\mu_s(t+t_s)t)}\,\sqrt{\frac{\pi}{2}}\,\mathrm{erf}(\frac{y_t}{\sqrt{2}})\right). \tag{50}$$

After substituting for $\mu_x(a_x)$ from Eq. (10) this formula is completely explicit.[20] Since Eq. (50) gives the correct dependence of $\Delta y'$ on y it includes effects nonlinear in y, such as island overlap and chaos, but this paper concentrates on small amplitudes where such effects are expected to be unimportant.

My procedure in using Eq. (50) has been to fix Q_x, Q_y, a_x and a_s and to increase ξ in steps until "instability" occurs. Note that for some "small enough" amplitude, for example $y_{\mathrm{min.}} = 0.001\sigma$, the equation is essentially linear and the motion is stable—the Courant-Snyder (CS) invariant of the motion even decays because $\delta > 0$. Furthermore Eq. (50) is *pseudohomogeneous* in the sense that $y_t = 0$ for all time is a solution, no matter how large ξ is. This makes it necessary to assign a small starting "seed" amplitude $y_{\mathrm{min.}}$, which may or may not grow due to parametric pumping. The "instability boundary" is defined as folows: as ξ is increased from zero, a smallest value $\xi_{\mathrm{min.}}$ is found for which $y_t > y_{\mathrm{max.}}$ for some value of t within a "large" number of turns, for example $N_t = 1000$; here, for example, $y_{\mathrm{max.}} = 0.1\sigma$ is an assigned "large" amplitude. (To partially suppress possible artificial correlations among Q, Q_x, and Q_s the parametric drive oscillations were given random starting t-indices in the range from 0 to -100. This is indicated by t_x and t_s in Eq. (50).) The value ξ determined in this way will be called $\xi_{\mathrm{sat.}}$ to distinguish it from the differently-calculated, single-resonance threshold $\xi_{\mathrm{thr.}}$. For most studies the definition of what constitutes "probable amplitudes" was taken to be the nine combinations of the points $a_x = 0.5\sigma_x, 1.5\sigma_x, 2.5\sigma_x$ and $a_s = 0.5\sigma_s, 1.5\sigma_s, 2.5\sigma_s$. Bringing this up to sixteen combinations by including $a_x = 3.5\sigma_x$ and $a_s = 3.5\sigma_s$ did not change the results markedly.

The procedure just described was performed for all points in the transverse tune plane, in steps of 0.01, for various choices of the other parameters. Results are shown in the following series of figures. Figure 6 shows results with synchrotron oscillations absent (i.e. $a_s = 0$) for $\delta = 10^{-4}$. The starting and instability-defining amplitudes here were $(y_{\mathrm{min.}}, y_{\mathrm{max.}}) = (0.001\sigma_y, 0.1\sigma_y)$; that is, instability was defined to mean parametric pumping from $\sigma_y/1000$ to $\sigma_y/10$. (Though the blow-up factor is large, the blown-up amplitude is relatively small.) In this and following figures the horizontal amplitude choices were $a_x = 0.5\sigma_x$, $a_x = 1.5\sigma_x$, and $a_x = 2.5\sigma_x$. At each point the worst case is plotted. By the *saturation principle* this gives the tune plane dependence of $\xi_{\mathrm{sat.}}$. In this case synchrotron oscillations are assumed to be absent. The most favorable region seems to be in the vicinity of $(Q_x, Q_y) = (0.40, 0.17)$ where $\xi_{\mathrm{sat.}} = 0.19$. Using the four quadrant symmetry in the fractional tune plane, equiv-

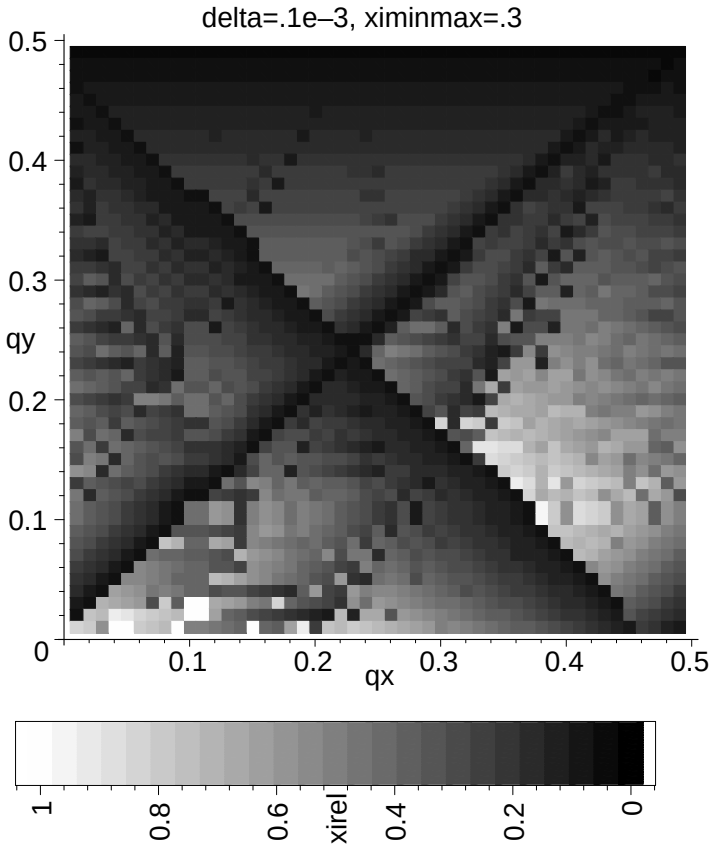

FIG. 6: For all points in one quadrant of the transverse tune plane the lowest value of $\xi_{\mathrm{sat.}}(a_x)$, for a representative sample of a_x-values, has been selected and plotted. In this and future cases the numerical value of $\xi_{\mathrm{sat.}}$ is to be obtained using the grayscale which multiplies the maximum value as recorded above (or below) the figure. (0.3 in this case.)

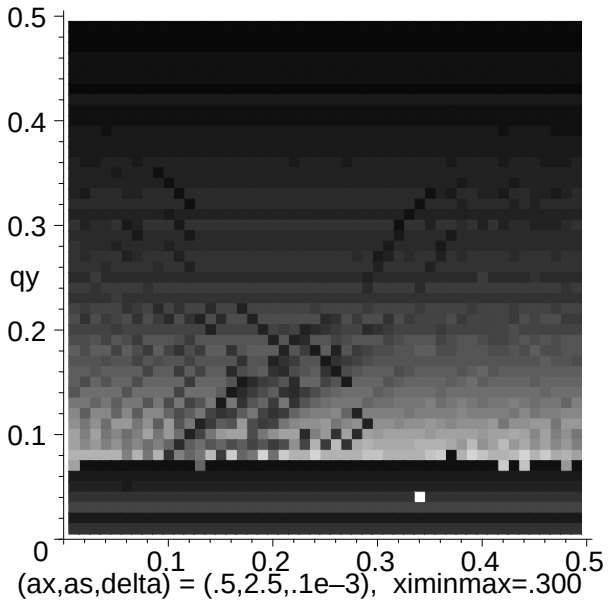

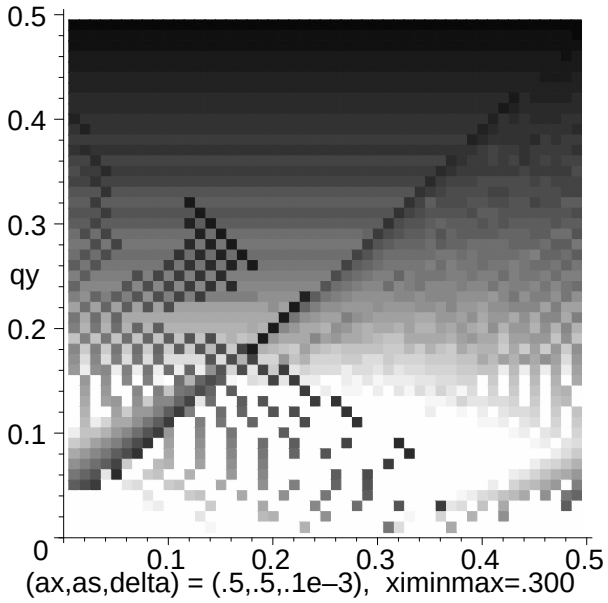

FIG. 7: For $\delta = 10^{-4}$, the tune plane dependence of $\xi_{\rm sat}$ is shown for a_s increasing from bottom to top in this column (and similarly in Figure 8 in the adjacent column) with a_x increasing in going from Figure 7 to Figure 8. The grayscale on the previous page is to be used to extract numerical values. According to the *saturation principle* the maximum specific luminosity at each point in the tune plane is obtained by picking the lowest value from a sufficiently comprehensive grid of data sets such as these.

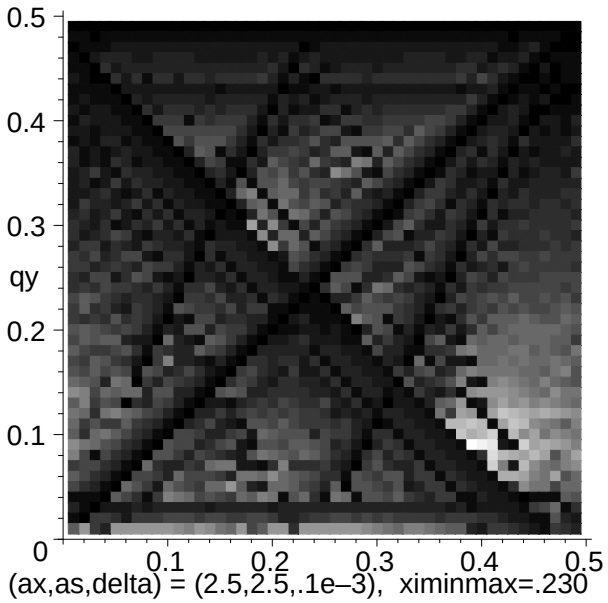

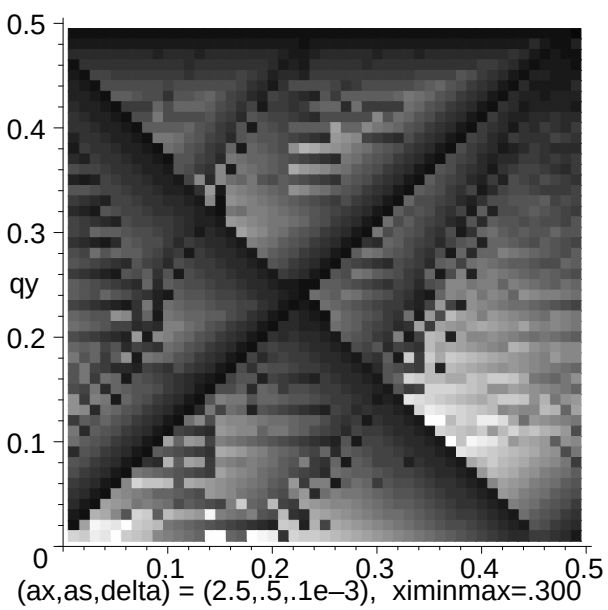

FIG. 8: The relationship of these figures to those in Figure 7 (in the adjacent column) is explained in the caption to Figure 7. The systematically superior performance on the more positive Q_x side of resonances is ascribed in section IV to the response illustrated in Figure 4

alent examples are $(Q_x, Q_y) = (0.40, 0.67)$, $(0.90, 0.17)$, and $(0.90, 0.67)$. (The two cases with $Q_y \approx 2/3$ may well be contraindicated for reasons unrelated to the present paper, but the "good regions" are probably larger than typical nonlinear stop band widths.)

The effect of the simultaneous presence of horizontal and longitudinal oscillation is shown in Figures 7 and 8, again for the case $\delta = 10^{-4}$. The synchrotronl amplitude a_s increases from bottom to top in steps of $2\sigma_s$ and the horizontal amplitude a_x increases from left to right in steps of $2\sigma_x$. The worst case values from these plots have been selected and plotted in Figure 9. Figure 10 is obtained similarly, but with $\delta = 10^{-2}$. Note the close similarity of these figures and therefore the comparatively weak dependence on δ. Apart from the modest increase of "maximin" value from 0.19 to 0.20 (shown at top of each plot) and a slightly "brighter" region in the lower right hand corner with $\delta = 10^{-2}$ the plots are qualitatively similar.

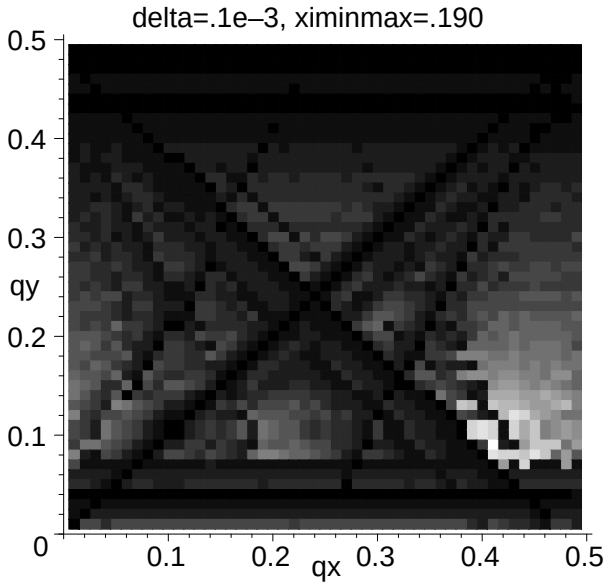

FIG. 9: At each point in the tune plane the worst case from a complete grid of data sets like those in Figures 7 and 8 is picked and plotted. $\delta = 0.0001$.

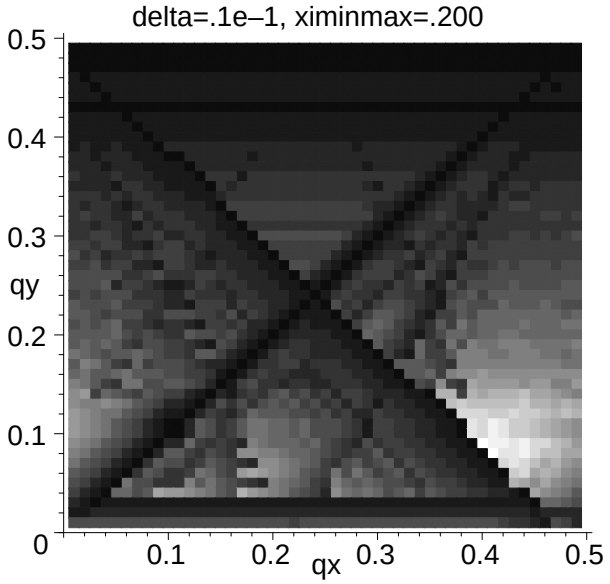

FIG. 10: At each point in the tune plane the worst case from data like that of Figures 7 and 8 but for $\delta = 0.01$ is picked and plotted. Comparing with Figure 9, note that the dependence on δ is weak over the entire tune plane.

VIII. COMPARISONS WITH EXISTING RINGS

Tune combinations for numerous existing colliding beam facilities are shown in Table III as well as in Figure 5. Most of the entries in the table come from Rice.[1] The column labeled $\Delta Q_{y,\mathrm{exp.}}$ contains the experimentally-determined quantity most directly comparable with $\xi_{\mathrm{th.}}$; (though it is determined indirectly) $\Delta Q_{y,\mathrm{exp.}}$ is the vertical tune shift of a minimum amplitude particle, including the effect of the perturbation of the beta function at the crossing point due to the beam-beam force. Theoretical values $\xi_{\mathrm{th.}}$ are determined by numerical iteration as explained in section VII. In most cases the (minimal) Monte Carlo aspect of the procedure results in no fluctuation in $\xi_{\mathrm{th.}}$; exceptions are noted by a ¶ symbol.

In constructing Table III, to account for multiple IP's, the tunes, as well as δ have been divided by the number of IP's, putting the calculation on a "per IP" basis. The measured LEP tune shifts, all with 4 IP's, fall far below the theoretical values and a PEP-6IP point, not shown, shows even greater disagreement. Within the assumptions of the current model these points should agree, absent reasons that invalidate the comparison. But even small ring asymmetries invalidate the per-IP basis. Usually in rings with multiple IP's the optics of the various IP's are not identical and the phase advances between IP's are not constant; these effects invalidate the present theory. Furthermore, since tune shifts from different IP's add directly, it is possible for the total tune shift in a ring with several IP's to approach 1/2 or even 1, and the implications of this have never been understood theoretically. Legitimate or not the more-than-2-IP theory to experiment ratios have therefore been dropped from the averaging which then yields theory/experiment equal to 1.26 ± 0.45. The 1-IP average is 1.12 ± 0.43

IX. PREDICTIONS AND CONCLUSIONS

Predictions based on Eq. (50) for the performance of various proposed rings are shown in Table IV. The entries labeled CESR-1.9 are for the "CESRc" reconfiguration of CESR, currently in progess.

As expected there is extreme sensitivity to tunes, including synchrotron tune Q_s. For CESR-1.9 the very high proposed value $Q_s \approx 0.11$ appears to limit $\xi_{\mathrm{th.}}$ seriously. Reducing Q_s (which is possible, at least in principle, for example with a third harmonic cavity) gives a big improvement. Choosing optimal tunes is even more important. In the full tune scans exhibited (as well as others not shown) the regions labeled "GOOD REGION"

TABLE III: Parameters of some circular, flat beam, e+e- colliding rings, and the saturation tune shift values predicted by Eq. (50). †From Brandt[3]. *Ion effect blow up of low energy beam may prevent beam-beam saturation; ¶Theory value is erratic. § Unequally-spaced IP's. For points not excluded by one of these factors the mean and standard deviations of theory/experiment (the last column) are 1.26 ± 0.45.

Ring	IP's	Q_x/IP	Q_y/IP	Q_s/IP	σ_s	β_y^*	$10^4\delta_y$	$\xi_{\rm th.}$	$\Delta Q_{y,\rm exp.}$	$\xi_{\rm th.}/\Delta Q_{y,\rm exp.}$
VEPP4	1	8.55	9.57	0.024	0.06	0.12	1.68	0.028	0.046	0.61
PEP-1IP	1	21.296	18.205	0.024	0.021	0.05	6.86	0.076	0.049	1.55
PEP-2IP	2	5.303	9.1065	0.0175	0.020	0.14	4.08	0.050	0.054	0.93
CESR-4.7	2	4.697	4.682	0.049	0.020	0.03	0.38	0.037	0.018	2.06
CESR-5.0	2	4.697	4.682	0.049	0.021	0.03	0.46	0.034	0.022	1.55
CESR-5.3	2	4.697	4.682	0.049	0.023	0.03	0.55	0.029	0.025	1.16
CESR-5.5	2	4.697	4.682	0.049	0.024	0.03	0.61	0.027	0.027	1.00
CESR-2000	1	10.52	9.57	0.055	0.019	0.02	1.113	0.028	0.043	0.65
KEK-1IP	1	10.13	10.27	0.037	0.014	0.03	2.84	0.046	0.047	0.98
KEK-2IP	2	4.565	4.60	0.021	0.015	0.03	1.42	0.048	0.027	1.78
LEP-46	4§	22.58	19.04	0.016	0.0076	0.05	0.958	0.128	0.034	
LEP-65	4§	22.57	19.04	0.019	0.009	0.05	2.7	0.086		
LEP-98	4§	24.59	24.05	0.029	0.0110	0.05	8.6	0.12¶	0.052	
PEP-LER	1	38.65	36.58	0.027	0.0123	0.0125	1.17	0.044	0.044	1.00
PEP-HER	1	24.57	23.64	0.045	0.0115	0.0125	1.98	0.056	0.026*	
KEK-LER	1	45.518	44.096	0.021	0.0057	0.007	2.34	0.042	0.032	1.31
KEK-HER	1	44.525	42.135	0.019	0.0055	0.007	2.18	0.060	0.018*	
BEPC	1	5.80	6.70	0.020	0.05	0.05	0.16	0.068	0.039	1.74

TABLE IV: Parameters of some proposed rings and the saturation tune shift values predicted by Eq. (eq:Numerical.1). In all cases $\sigma_s = \beta_y^*$. The dependencies are far too complicated to be faithfully represented by such a limited set of data and small changes of tunes may yield substantially different values of $\xi_{\rm th.}$. ¶Theory value is erratic.

Ring	IP's	Q_x/IP	Q_y/IP	Q_s/IP	$10^4\delta_y$	$\xi_{\rm th.}$
CESR-1.9	1	10.52	9.57	0.11	0.55	0.016¶
	1			0.03		0.026
	1			0.0		0.022
	1	10.42	9.17	0.11		0.030
	1			0.03		0.096
	1			0.0		0.100
VLLC(e)	1	.59	.05	0.11	100	0.044
	1			0.03		0.104
	1			0.0		0.098
VLHC(p)	1	.59	.05	0.03	1.0e-8	0.056

in Figure 5 appear to be more promising than other regions. And yet, as least as far as cases documented in Table III, these regions have never been tried operationally. Even within the present model there is resonant structure within these regions and effects not included, especially nonlinear resonances, would make it necessary to probe around for best operating points. For starters the fact that $Q_y = 0.67$ sits exactly on third integer resonance would seem to contraindicate the upper two quadrants. But the so-called "good regions" are considerably larger than typical nonlinear stop bands, so the "good regions" in all four quadrants are candidates for good performance.

The location of good regions has been explained in this paper by the parametric resonator response illustrated in Figure 4. Amplitude build-up occurs preferentially on the negative Q_x side of resonances.[21] Those resonances expected to be important in Table II are in fact visible in the tune plane plots, such as Figure 8. Including synchrotron oscillations complicates the pattern considerably and favors low Q_s.

If one accepts the *saturation principle* and the numerical results of this paper there is potential for *large* increase in specific luminosity compared to existing operating points. Unfortunately large specific luminosity does not guarantee large maximum luminosity, as nonlinear effects may limit the amount by which the beam currents can be increased above their threshold values. If the total beam current is limited, there may be favorable compromises, using more, but smaller, bunches, to exploit high specific luminosity.

For VLLC(e), (Very Large Lepton Collider) entries in Table IV the tunes have arbitrarily been taken to be the same as for LEP-98 even though more favorable points exist (within the present model.) The achievable tune shift values are consistent with projections by Sen, Norem and others,[9] even though the extrapolation procedure on which their values were based has been argued to be invalid.

The damping decrements δ of hadron colliders are some ten orders of magnitude less than for electron machines. In spite of this big factor the maximum beam-beam tune shifts in proton machines are typically one tenth of those in electron machines. For this reason, because δ has been thought to be important, it has usually been thought that entirely different mechanisms must be responsible for the limits. One effect contributing to the (relatively)

large value ξ values achieved in proton machines is the fact that their beams are round rather than flat. But the (relatively) large ξ value may also be partly explained by the relatively weak δ dependence claimed in the present paper. To pursue this line of reasoning, the bottom entry of Table IV shows the result of applying the formulas of this paper to the Very Large Hadron Collidr VLHC(p). Comparing with the second VLLC(e) entry, changing the value of δ by ten orders of magnitude, only alters ξ by factor 0.54. This is consistent with a dependence $\xi \sim \delta^{0.06}$. Since this is not inconsistent with the dependence observed in electron machines (Figure 2) it is possible that the physics of the beam-beam interaction may be much the same in proton as in electron colliding rings. If so, the luminosities of next-generation proton colliders may be much greater than current projections suggest. That said, the value $\xi_{\rm th.} = 0.056$ given in the table for VLHC(p) is undoubtedly too optimistic; other effects, such as diffusive beam growth, which depends strongly on δ, are likely to overwhelm the parametric pumping effect on which Table IV is based.

APPENDIX A: EXCITATION OF VERTICAL BETATRON MOTION BY AN EXTERNAL SHAKER

To illustrate the difference equation method it will be used in this section to calculate the vertical motion induced by the "direct drive" due to an external "shaker". As well as introducing the method of analysis, the equations of motion and an example of aliasing, this introduces the important damping decrement δ_y and shows how it influences the motion. (But the influence of δ_y on parametric drive need not be the same.)

The deflection caused by the external drive on the t'th turn is

$$\Delta y'_t = F_E \cos \mu_E t. \tag{A1}$$

We postulate a small "damping decrement" δ_y, so that the once-around transfer map in "Twiss form" is

$$\begin{pmatrix} y \\ y' - \Delta y'/2 \end{pmatrix}_{t+1} = \exp(-\delta_y) \times \\ \times \begin{pmatrix} C_y + \alpha_y S_y & \beta_y S_y \\ -\gamma_y S_y & C_y - \alpha_y S_y \end{pmatrix} \begin{pmatrix} y \\ y' + \Delta y'/2 \end{pmatrix}_t, \tag{A2}$$

and a similar equation can be written for backwards propagation from t to $t-1$. Note that y' is evaluated at the middle of the shaker. We are using the notation $C_y \equiv \cos \mu_y$ and $S_y \equiv \sin \mu_y$ and are intentionally using the subscript t as a turn index to be suggestive of the time measured in units of the revolution period. It will however always be an integer. Proceeding as in the derivation of Eq. (5) yields

$$y_{t+1} - 2C_y y_t + y_{t-1} = \beta_y S_y \Delta y'_t - \delta_y (y_{t+1} - y_{t-1}). \tag{A3}$$

After solving this for y_t it will be possible to obtain y'_t from the equation

$$y'_t = \frac{y_{t+1} - y_{t-1} - 2\alpha_y S_y y_t + \delta_y (y_{t+1} + y_{t-1})}{2\beta_y S_y}. \tag{A4}$$

As usual with driven oscillations we expect a response at the drive frequency. i.e.

$$y_t = A \cos \mu_E t + B \sin \mu_E t, \tag{A5}$$

where any "transient" (i.e. any solution of the homogeneous equation which is obtained by setting the drive term of Eq. (A3) to zero.) has been neglected. In electron accelerators this neglect is justified by the existence of true damping. Even in proton accelerators where true damping is negligible, it can be justified by decoherence, or, as it is also called, Landau damping. Substituting into Eq. (A3) and equating the "in-phase" and the "out-of-phase" coefficients separately to zero, one obtains

$$\begin{aligned} A &= \tfrac{\beta_y S_y (C_E - C_y)/2}{(C_E - C_y)^2 + \delta_y^2 S_E^2} F_E, \\ B &= \tfrac{\beta_y S_y S_E \delta_y/2}{(C_E - C_y)^2 + \delta_y^2 S_E^2} F_E. \end{aligned} \tag{A6}$$

For near-resonance analysis we define[22][23]

$$\varepsilon = \mu_E - \mu_y \tag{A7}$$

Substituting into Eq. (A5) and neglecting terms containing $\varepsilon \delta_y$ we obtain

$$\begin{aligned} y_t &= \tfrac{F_E \beta_y/2}{\varepsilon^2 + \delta_y^2} \left[-\varepsilon \cos \mu_E t + \delta_y \sin \mu_E t \right] \\ &= -\tfrac{F_E \beta_y}{2\sqrt{\varepsilon^2 + \delta_y^2}} \cos(\mu_E t + \phi), \end{aligned} \tag{A8}$$

where $\phi = \tan^{-1}(\delta_y/\varepsilon)$, $\sin\phi = \delta_y/\sqrt{\varepsilon^2 + \delta_y^2}$, and $\cos\phi = \varepsilon/\sqrt{\varepsilon^2 + \delta_y^2}$. Taking $\alpha_y = 0$, the slope is given by

$$\begin{aligned} y'_t &= \tfrac{F_E/2}{\varepsilon^2 + \delta_y^2} \left(\delta_y \cos \mu_E t + \varepsilon \sin \mu_E t \right) \\ &= \tfrac{F_E}{2\sqrt{\varepsilon^2 + \delta_y^2}} \sin(\mu_E t + \phi). \end{aligned} \tag{A9}$$

These equations should be reminiscent of driven simple harmonic motion though they are the solution of the difference equations Eq. (A2). Except nearly on resonance, the "in-phase" $\cos \mu_E t$ term of Eq. (A8) is dominant, but for small ε, the "out-of-phase" $\sin \mu_E t$ dominates. The response always "lags", with phase angle ϕ varying from zero to $-\pi$ as the drive frequency varies from zero to infinity. With $\phi = -\pi/2$ at resonance, the response changes sign in passing from below to above the resonance. The Courant-Snyder (CS) invariant of the motion is

$$\epsilon_{y,CS} = \frac{\beta_y F_E^2/4}{\varepsilon^2 + \delta_y^2}. \tag{A10}$$

For small deflections the averaged change in $\epsilon_{y,CS}$ due to the shaker is

$$\begin{aligned}\langle \Delta\epsilon^{(S)}_{y,CS}\rangle &\approx \langle 2y'_t \Delta y'_t\rangle \\ &= \langle \tfrac{\beta_y F_E}{\varepsilon^2+\delta_y^2}\,(\delta_y \cos\mu_E t + \varepsilon \sin\mu_E t)\, F_E \cos\mu_E t\rangle \\ &= \tfrac{\beta_y F_E^2 \delta_y/2}{\varepsilon^2+\delta_y^2}. \end{aligned} \tag{A11}$$

The averaged *fractional* change is therefore

$$\frac{\langle \Delta\epsilon^{(S)}_{y,CS}}{\epsilon_{y,CS}\rangle = 2\delta_y}\ . \tag{A12}$$

This can be compared to the fractional change due to damping

$$\frac{\Delta\epsilon^{(D)}_{y,CS}}{\epsilon_{y,CS}} = -2\delta_y. \tag{A13}$$

The fact that these changes are equal but opposite is consistent with the equilibrium.

APPENDIX B: HIGHER ORDER PARAMETRIC RESONANCES

From Eq. (A3) the equation of motion is

$$y_{t+1}(1-\delta) - 2Cy_t + y_{t-1}(1+\delta) = \beta S \Delta y'_t(x_t, y_t). \tag{B1}$$

Here quantities without subscripts (β, μ, $C \equiv \cos\mu_y$, $S \equiv \sin\mu_y$ and δ) implicitly refer to y-motion. Eq. (14) was not the most general possibility for parametric resonance; let us seek a solution of the form[24] [25]

$$y_t = \sum_m a_m \exp m\tilde{\mu} t, \tag{B2}$$

where $\tilde{\mu} = \mu + \varepsilon$ is "close to" μ in a sense to be spelled out below. The phase advance $\tilde{\mu}$ can be shifted by an integral multiple of 2π without altering Eq. (B2). Actually there is further degeneracy. The replacement $\mu \to \mu + \pi$ is equivalent to reversing the signs of both C and S. This reverses the signs of the y and y' outputs from the one-turn map around the storage ring. Since the deflection $\Delta y'_t$ is an odd function of y_t, the next beam-beam deflection is also reversed. This means that the replacement $\mu \to \mu + \pi$ is equivalent to toggling the sign of y_t every turn so the y-axis points up for t even and down for t odd. The phase advance $\tilde{\mu}$ can therefore be shifted by $h\pi$ (h being an integer) without altering Eq. (B1). We therefore permit arbitrary half integer additions to or subtractions from μ but require μ and $\tilde{\mu}$ to have the same "fractional parts",

$$0 \le \mu_{\rm frac.}, \tilde{\mu}_{\rm frac.} < \pi,\ \tilde{\mu} = \mu + \varepsilon,\ \text{where } \tilde{\mu} - \tilde{\mu}_{\rm frac.} = \mu - \mu_{\rm frac.}. \tag{B3}$$

Here the term "fractional" has been generalized to mean "modulo half-integers". A resonance condition will presumably be met for ε sufficiently close to zero. This being a "variation of constants" method, the coefficients a_m are to be permitted to vary, but only *slowly* with time. Furthermore, since we are seeking "normal modes" of the system, they are assumed to have the common time dependence $\exp(i\omega t)$. Therefore Eq. (B2) yields

$$\begin{aligned} y_{t+1} &= \textstyle\sum_m a_m (1+i\omega)\, e^{im\tilde{\mu}}\, e^{im\tilde{\mu}t}, \\ y_{t-1} &= \textstyle\sum_m a_m (1-i\omega)\, e^{-im\tilde{\mu}}\, e^{im\tilde{\mu}t}. \end{aligned} \tag{B4}$$

Suppressing the summation over n, Eq. (16) now takes the form

$$\frac{-\Delta y'_t}{4\pi\xi/\beta}\,\frac{2}{B_n} = \sum_m a_m \quad [\exp(i(2n\mu_x + m\tilde{\mu})t) + \\ + \exp(i(-2n\mu_x + m\tilde{\mu})t)]. \tag{B5}$$

Like μ, μ_x is subject to degeneracy; for arbitrary integer k, we define $0 \le \mu_{x,\rm frac.} < \pi$, and permit $\mu_x = k\pi + \mu_{x,\rm frac.}$. Again the fractional parts are defined modulo half-integers. In this case the degeneracy is due to the fact that the deflection is an even function of x. When longitudinal motion is included there is a similar degeneracy in the choice of Q_s. In simulating performance I will simply take Q_s to be fixed at a "small" value of order 0.1 or less.[26] The fractional ranges to be investigated are therefore

$$0 < Q_x < 0.5, \quad 0 < Q < 0.5, \quad Q_s = \text{fixed}. \tag{B6}$$

The other three quadrants of modulo-integer fractional tunes will be identical. A "resonance condition" takes the form

$$2n\mu_x = \pm(2+s)\tilde{\mu}, \quad \text{or, for } n \ne 0, \quad \mu_x = \pm\frac{2+s}{2n}\,(\mu+\varepsilon), \tag{B7}$$

where s is a positive or negative integer. The integers h and k entering μ and μ_x to permit this condition to be satisfied are not in general the same. The tune degeneracies will be reflected by the fact that the coefficients in the equations are sinusoidal functions of the tunes and are therefore invariant to certain translations of the tunes. Also there is other redundancy. For example the replacement $s \to -4 - s$ has the same effect as an overall sign change.

It is these degeneracies (also known as "aliasing") which make the spectrum of resonances "richer" than is the spectrum of resonances of the Mathieu equation. Any particular resonance can be identified by a (non-unique) combination of h, k, s, $\pm$. Even two different values of n can contribute to the same resonance, in which case two different values of B_n will enter the solution. The various ambiguities can, to some extent, be hidden, and a particular resonance isolated, by re-expressing the (externally controllable) parameter μ_x in terms of ε, as in the second of Eqs. B7), allowing s to take all values except -2 (in which case there is no time varying parametric drive) and requiring $\varepsilon << 1$.

Using Eq. (B7) the r.h.s. of Eq. (B1) can be manipulated into the form

$$-2\pi\xi\, SB_n \sum_m (a_{m-2-s} + a_{m+2+s})\, \exp(im\tilde{\mu}t). \quad \text{(B8)}$$

Substituting into Eq. (B1), dropping (small) terms containing $\omega\delta$ and setting the coefficients of $\exp(im\tilde{\mu}t)$ individually to zero yields, for $-\infty < m < \infty$,

$$\begin{aligned}((1 + i\omega - \delta)\ \ & e^{im\bar{\mu}} - 2C + (1 - i\omega + \delta)\, e^{-im\bar{\mu}})a_m \\ & = -2\pi\xi\, SB_n\, (a_{m-2-s} + a_{m+2+s}). \quad \text{(B9)}\end{aligned}$$

These equations reduce to

$$\begin{aligned}(\tilde{C}_m - C - \omega'\tilde{S}_m)\, a_m & \\ = -\pi\xi SB_n\, (a_{m-2-s} + a_{m+2+s}), & \quad \text{(B10)}\end{aligned}$$

where some abbreviations have been introduced;

$$\begin{aligned}\omega' &\equiv \omega - i\delta, \\ \tilde{S}_j &\equiv \sin j\tilde{\mu} \equiv \sin j(\mu + \varepsilon), \\ \tilde{C}_j &\equiv \cos j\tilde{\mu} \equiv \cos j(\mu + \varepsilon). \quad \text{(B11)}\end{aligned}$$

For any particular integer $s \neq 2$ and any positive integer n, Eqs. (B10) form an infinite set of equations, one for each integer m. To truncate this set we pick an arbitrarily large positive integer M and retain only the equations for $-M < m < M$;[27]

$$\begin{aligned}(\tilde{C}_M - C - \omega'\tilde{S}_M)\, a_M &= -\pi\xi SB_n\, (a_{M-2-s} + a_{M+2+s}), \\ (\tilde{C}_{M-1} - C - \omega'\tilde{S}_{M-1})\, a_{M-1} &= -\pi\xi SB_n\, (a_{M-3-s} + a_{M+1+s}), \\ &\cdots \\ (\tilde{C}_1 - C - \omega'\tilde{S}_1)\, a_1 &= -\pi\xi SB_n\, (a_{-1-s} + a_{3+s}), \\ (1 - C)\, a_0 &= -\pi\xi SB_n\, (a_{-2-s} + a_{2+s}), \\ (\tilde{C}_1 - C + \omega'\tilde{S}_1)\, a_{-1} &= -\pi\xi SB_n\, (a_{-3-s} + a_{1+s}), \\ &\cdots \\ (\tilde{C}_{M-1} - C + \omega'\tilde{S}_{M-1})\, a_{-M+1} &= -\pi\xi SB_n\, (a_{-M-1-s} + a_{-M+3+s}), \\ (\tilde{C}_M - C + \omega'\tilde{S}_M)\, a_{-M} &= -\pi\xi SB_n\, (a_{-M-2-s} + a_{-M+2+s}). \quad \text{(B12)}\end{aligned}$$

Coefficients with indices outside the range $-M < m < M$ are to be set to zero. Since these are linear, homogeneous equations, the solvability of the equations is governed by the determinant Δ of the matrix formed from their coefficients. Some properties of Δ can be obtained using a special case, $M = 2, s = 0$, as a model;

$$\Delta(\mu, \varepsilon, \omega'^2, \xi^2) = \det \begin{vmatrix} \tilde{C}_2 - C - \omega'\tilde{S}_2 & 0 & \pi\xi SB_n & 0 & 0 \\ 0 & \tilde{C}_1 - C - \omega'\tilde{S}_1 & 0 & \pi\xi SB_n & 0 \\ \pi\xi SB_n & 0 & 1 - C & 0 & \pi\xi SB_n \\ 0 & \pi\xi SB_n & 0 & \tilde{C}_1 - C + \omega'\tilde{S}_1 & 0 \\ 0 & 0 & \pi\xi SB_n & 0 & \tilde{C}_2 - C + \omega'\tilde{S}_2 \end{vmatrix}. \quad \text{(B13)}$$

Since the a_0 equation does not depend on ω', it can be solved for a_0 which can then be eliminated from the other equations. Reversing the sign of M obviously leaves the equations invariant, but the following observation is more essential: Just reversing the signs of the indices (e.g. $a_m \equiv b_{-m}$) can, on the one hand, not alter the solvability of the equations and, on the other hand, produces the same set of equations except with the sign of ω' reversed. It follows that the characteristic determinant is a function only of ω'^2. That Δ depends only on ξ^2 can be inferred by multiplying both one row, say the second, and the corresponding column by -1. This is equivalent to reversing the sign of ξ but leaving the equations and the determinant otherwise unaltered. Because Δ is a function only of $(\omega - i\delta)^2$, the substitution $\omega' = -i\delta$ yields $\Delta(\mu, \varepsilon, -\delta^2, \xi^2)$, a polynomial in δ^2 and ξ^2 with all coefficients real.

The simplest example of Eqs. (B12) has $s = 0$, $M = 1$. Dropping the $m = 0$ equation (because it does not contribute to lowest order) yields

$$\begin{aligned}(\tilde{C}_1 - C - \omega'\tilde{S}_1)\, a_1 &= -\xi S\, (a_{-1} + \hat{a}_3), \\ (\tilde{C}_{-1} - C - \omega'\tilde{S}_{-1})\, a_{-1} &= -\xi S\, (\hat{a}_{-3} + a_1). \quad \text{(B14)}\end{aligned}$$

Terms to be dropped because they bring in coefficients outside the range being retained are indicated with circumflexes ($\hat{}$). (The rationale behind this approximation is that the retained terms a_1 and a_2 describe the

dominant vertical motion, perturbed only in lowest order by the parametric pumping. Since neither of these coefficients appears in the $m = 0$ equation, that equation can be dropped—the error made is "higher order" in the small parameter $\pi\xi SB_n$.) Continuing with the example, the condition to be satisfied for homogeneous Eqs. (B14) to have a nontrivial solution is

$$\det \begin{vmatrix} \tilde{C}_1 - C - \omega'\tilde{S}_1 & \xi S \\ \xi S & \tilde{C}_1 - C + \omega'\tilde{S}_1 \end{vmatrix} = 0. \qquad \text{(B15)}$$

From Eq. (B3) which defined ε, we can approximate $\tilde{C}_1 \approx C - \varepsilon S$, $\tilde{S}_1 \approx S$, to get

$$(\omega - i\delta)^2 = \varepsilon^2 - \xi^2. \qquad \text{(B16)}$$

This agrees with Eq. (23) and is even a slight improvement in that the damping has been handled explicitly and does not need to be inserted "by hand". Expressed in terms of system parameters using Eqs. (B2) and (B7), the motion is stable if

$$\Re\sqrt{\xi^2 - (\frac{2n\mu_x}{2+0} - \mu)^2} < \delta. \qquad \text{(B17)}$$

If $\delta = 0$ (no damping) the limits of the band of unstable motion are obtained more directly by setting $\omega' = 0$ in Eq. (B15);

$$\begin{vmatrix} \tilde{C}_1 - C & \xi S \\ \xi S & \tilde{C}_1 - C \end{vmatrix} = 0, \quad \text{or} \quad -\xi < \varepsilon < \xi. \qquad \text{(B18)}$$

To obtain a more accurate formula (for the same $s = 0$ resonance) one must retain more terms. (For this case the determinant needed for the next approximation was already exhibited in Eq. (B13).) In general, after eliminating a_0, there are $2M$ equations in $2M$ unknowns. For fixed n, s and μ, the determinant is a function of ε and ξ. The vanishing of the determinant formed from the coefficients determines the stability boundaries in the (ε, ξ) parameter space.

The stability of motion can be formulated in terms of the eigenvalues of a matrix. To illustrate this, and to exhibit a different resonance, consider the case $s = 1$, $M = 2$. In this case the central equation can be dropped (to lowest order) since it does not "couple" a_0 to any of the retained coefficients. Solvability requires the vanishing of the determinant

$$\det \begin{vmatrix} (\tilde{C}_2 - C)/\tilde{S}_2 - \omega' & 0 & \xi S/\tilde{S}_2 & 0 \\ 0 & (\tilde{C}_1 - C)/\tilde{S}_1 - \omega' & 0 & \xi S/\tilde{S}_1 \\ -\xi S/\tilde{S}_1 & 0 & -(\tilde{C}_1 - C)/\tilde{S}_1 - \omega' & 0 \\ 0 & -\xi S/\tilde{S}_2 & 0 & -(\tilde{C}_2 - C)/\tilde{S}_2 - \omega' \end{vmatrix} = 0. \qquad \text{(B19)}$$

The four solutions of this equation for ω' are the exponents of the possible homogeneous motions of the system. The elements of this matrix have been obtained by reading coefficients directly from Eq. (B12). For fixed n, s and μ, since $\tilde{\mu} = 2n\mu_x/(1+s)$, each of these eigenvalues is a function of μ_x and ξ_n. Unstable regions of the (μ_x, ξ_n) parameter space are characterized by at least one of these eigenvalues having a positive real part.

Since instability boundaries are marked by the vanishing of Δ for $\omega = 0$, we will be interested primarily in the case of "small" ξ and δ. We therefore define an expansion[28]

$$\Delta(\mu, \varepsilon, -\delta^2, \xi^2) = \Delta_{00}(\mu,\varepsilon) + \Delta_{10}(\mu,\varepsilon)\xi^2 + \Delta_{01}(\mu,\varepsilon)\delta^2 + \Delta_{11}(\mu,\varepsilon)\xi^2\delta^2 + \ldots. \qquad \text{(B20)}$$

This series terminates; the termination depends on M which is fixed. Because of the aliasing discussed previously, Eq. (B20) has a very complicated "global" dependence on ε. To help in identifying "local" resonances, and because we cannot simply set $\varepsilon = 0$, we must also expand for small ε.

$$\begin{aligned}\Delta(\mu, \varepsilon, -\delta^2, \xi^2) = \; & \Delta_{100}(\mu)\xi^2 + \Delta_{010}(\mu)\delta^2 + \Delta_{110}(\mu)\xi^2\delta^2 + \cdots + \Delta_{101}(\mu)\xi^2\varepsilon + \Delta_{011}(\mu)\delta^2\varepsilon + \Delta_{111}(\mu)\xi^2\delta^2\varepsilon + \cdots + \\ & + \Delta_{002}(\mu)\varepsilon^2 + \Delta_{102}(\mu)\xi^2\varepsilon^2 + \Delta_{012}(\mu)\delta^2\varepsilon^2 + \Delta_{112}(\mu)\xi^2\delta^2\varepsilon^2 + \ldots \end{aligned} \qquad \text{(B21)}$$

There is no leading term $\Delta_{000}(\mu, \varepsilon)$ since that term corresponds to the absence of perturbation. The coefficient $\Delta_{001}(\mu, \varepsilon)$ also vanishes since, in the no perturbation limit, Δ is an even function of ε.

The Δ's are trigonometric functions of μ. They are plotted as functions of μ in Figure 11. Some sample

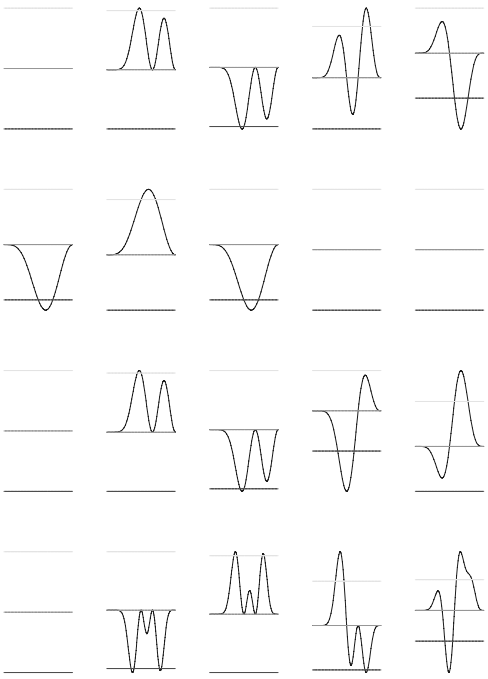

FIG. 11: Δ_{100} Δ_{002} Δ_{010} Δ_{101} Δ_{110}, in that order from left to right, are plotted on the range $0 < \mu < \pi$. Vertically, starting at the top, the plots correspond to $s = -1, 0, 1, 2$ with $M = s + 1$. Horizontal grid lines mark -1,0,1. All functions are either even or odd about $\mu = \pi$.

formulas for $M = 1$, $s = 0$ are

$$\begin{aligned} \Delta_{010} &= (-2 + \cos\mu + 2\cos 2\mu - \cos 3\mu)/4, \\ \Delta_{011} &= (\sin\mu - 2\sin 2\mu + \sin 3\mu)/2, \end{aligned} \tag{B22}$$

and for $M = 2$, $s = 0$ the corresponding formulas for Δ_{010} and Δ_{011} are

$$\begin{aligned} 16\Delta_{010} &= -6 + 3\cos\mu + 4\cos 2\mu + 2\cos 3\mu - 2\cos 4\mu \\ &\quad -4\cos 5\mu + 4\cos 6\mu - \cos 7\mu, \\ 8\Delta_{011} &= (-3\sin\mu - 6\sin 2\mu + 2\sin 3\mu + 2\sin 4\mu \\ &\quad +8\sin 5\mu - 10\sin 6\mu + 3\sin 7\mu. \end{aligned} \tag{B23}$$

This shows that the coefficients themselves do not "get small" as M is increased. Their magnitudes roughly correspond to setting ξ, δ and ε approximately 1, settings which are all far beyond the range of applicability of the theory. There seems, therefore, to be no value in picking M any larger than is necessary to retain a term proportional to ξ in the outermost rows and columns of the fundamental matrix; in other words, $M = |s| + 1$.

The very complicated dependencies of the coefficients on μ will (presumably) cause the resonance strengths to exhibit erratic global variation. This complication can be hidden formally by treating the Δ_{ijk} coefficients as constants; i.e. by holding μ fixed. For example, as ξ increases from zero, with ε sufficiently small, a "nearby" instability boundary is encountered for

$$\xi^2 = -\frac{\Delta_{002}\varepsilon^2 + \Delta_{010}\delta^2 + (\Delta_{011}\varepsilon + \Delta_{012}\varepsilon^2)\delta^2}{\Delta_{100} + \Delta_{101}\varepsilon + \Delta_{110}\delta^2 + \Delta_{102}\varepsilon^2 + (\Delta_{111}\varepsilon + \Delta_{112}\varepsilon^2)\delta^2}. \tag{B24}$$

The leading part of the denominator, $\Delta_{100} + \Delta_{101}\varepsilon$, is either negative or can be made negative by choosing the appropriate sign for ε; then the overall expression is positive (for sufficiently small δ) in those cases for which $\Delta_{002} > 0$. This makes ξ real which implies true resonance, at least in this case, and there are other possibilities.

To study the resonances in greater detail it is appropriate to proceed in close analogy with traditional treatments of the Mathieu equation. That is, holding μ and δ fixed, let us plot ε as a function of ξ for the curve or curves separating stable and unstable regions, as they emanate from the origin ($\xi = \varepsilon = 0$). For this purpose an expansion more compact than Eq. (B21) is (suppressing μ and δ arguments)

$$\Delta_{\mu,\delta}(\varepsilon, \xi) = \Gamma_0(\xi) + \Gamma_1(\xi)\varepsilon + \Gamma_2(\xi)\varepsilon^2 + \ldots \tag{B25}$$

These coefficients $\Gamma_i(\xi)$ are obtained simply from the $\Delta_{ijk}(\mu)$ coefficients defined previously. Setting $\Delta = 0$ and solving Eqs. (B25) (keeping only the terms shown) yields

$$\varepsilon_{\mu,\delta}(\xi) = \frac{-\Gamma_1(\xi) \pm \sqrt{\Gamma_1^2(\xi) - 4\Gamma_2(\xi)\Gamma_0(\xi)}}{2\Gamma_2(\xi)}. \tag{B26}$$

The dependence of these roots $\varepsilon_{\mu,\delta,\pm}$ on ξ for particular values of δ and μ are plotted in Figure 12. Values of ξ for which the roots are complex do not show up on these plots. This plot is strikingly similar to the plot of the instability boundaries of the Mathieu equation.[6]

The "threshold value" $\xi_{\text{thr.}}$ satisfies

$$\Gamma_1^2(\xi_{\text{thr.}}) - 4\Gamma_2(\xi_{\text{thr.}})\Gamma_0(\xi_{\text{thr.}}) = 0. \tag{B27}$$

[1] D. Rice, Cornell Report CBN 01-09 (2001) CESRc PAC report, June (2001) and private communication

[2] J. Seeman, Springer-Verlag Lecture Notes in Physics 247, Nonlinear Dynamics Aspects of Particle Accelerators, Sardinia, 121 (1985)

[3] D. Brandt et al., Rep. Prog. Phys. **63** 939 (2000)

[4] E. Keil and R. Talman, Part. Accel. **14**, 109 (1983)

[5] Lord Rayleigh, *Complete Scientific Papers,* **2**, 88 (1883), **3**, 1 (1887). Dover reprint (1964)

[6] N. McLachlan, *Theory and Application of Mathieu Functions,* Dover (1964)

[7] L. Landau and E. Lifshitz, *Mechanics*, Butterworth-

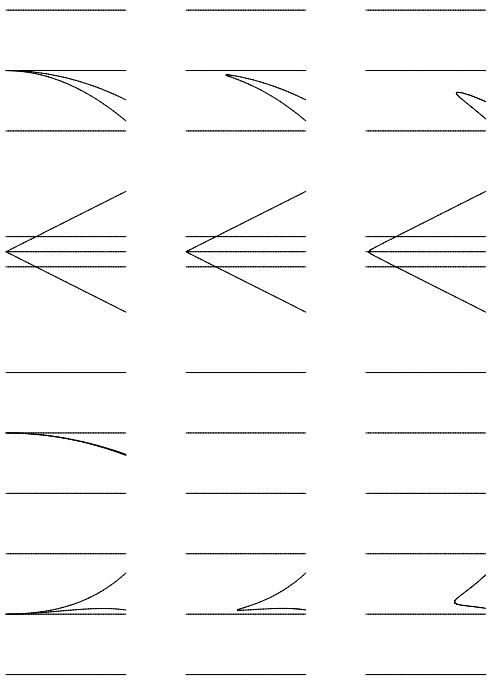

FIG. 12: $\varepsilon_\pm(0)$ $\varepsilon_\pm(1/1000)$ $\varepsilon_\pm(1/200)$ The edges of instability bands, are plotted on the range $0 < \xi < 0.2$, where ξ is the abcissa and ε is the ordinate. Vertically arrayed, starting at the top, the plots correspond to $s = -1, 0, 1, 2$ with $M = s + 1$. Horizontally arrayed, the damping decrements are $\delta = 0, 1/1000, 1/200$, as indicated in parenthesis. The vertical phase advance for this plot is $\mu_y = 0.57 \times 2\pi$. Horizontal lines mark $\varepsilon = -0.05, 0, 0.05$. For the dominant $s = 0$ resonance (second from top) the displacement of the threshold away from $\xi = 0$ is just barely visible for $\delta = 1/200$ and the stop band width is proportional to ξ, as is true for the Mathieu equation. For higher order stop bands the threshold dependence on δ is much stronger and the power of the power law dependence increases as the order increases. These features are also exhibited by the Mathieu equation with damping.

Heinemann, Oxford, 1976, p. 80 (1976)

[8] V. Migulin, editor, *Basic Theory of Oscillations*, Mir Publishers, Moscow (1983)

[9] T. Sen and J. Norem, *Proceedings of the Workshop on an e+e- Collider in the VLHC Tunnel,* Chicago, Fermilab preprint, 2001 http://fnalpubs.fnal.gov./archive/2001/conf/Conf-01-107-T.html

[10] The assumption of negligible beam height uses the result that synchrotron-radiated photons are emitted precisely in the forward direction; since their typical angle is $1/\gamma$ this is an excellent, but not perfect assumption.

[11] The instability to be described causes non-destructive growth to a well-defined amplitude, *not* unlimited exponential growth. Therefore the term "barely stable" in the "saturation principle" could more accurately be replaced by "barely unstable at zero amplitude". In the picture being promoted most of the particles are oscillating more or less stably (with random, uniformly distributed, phases) at the amplitudes to which they have been pumped. The amplitude of any particle that "loses lock" from its own pumping decays toward zero until the particle gets caught up again.

[12] From here on in this paper quantities without subscripts, such as ξ, β, Q and σ, will implicitly refer to y motion. The one exception, to avoid a clash of symbols later on, will be a_y.

[13] The beam-beam deflection also depends on horizontal position x and longitudinal position s; these dependencies will be incorporated later.

[14] "Tunes" Q and phase advances per turn $\mu = 2\pi Q$ will be interchanged as convenient, and without warning, and either may be referred to as a "frequency".

[15] The fact that Eq. (5) generalizes the Mathieu equation can be seen by re-expressing it as $(y_{t-1} + y_{t+1} - 2y_t) + \delta(y_{t+1} - y_{t-1}) + 2(1 - C_y)y_t + \beta S_0 \Delta y'(t) = 0$. In the so-called "smooth approximation" (fractional changes per turn assumed small) the first term reduces to $\ddot{y}$, and the second to $2\delta\dot{y}$, the "damping" term in simple harmonic motion. The term $2(1 - C_y)y_t$ generalizes the "restoring force" term. The term $\beta S_0 \Delta y'$, proportional to y_t for small y_t, makes the system nonautonomous through its dependence on x_t and s_t, and provides the parametric drive.

[16] The dependence on amplitude a has been incorporated into the *ad hoc* factor $(1 - \exp(-a^2/\sigma^2))$ in Eq. (8) has been included in Eq. (8) to recover the correct tune shift at large a while retaining the leading ($\sim a^2$) behavior.

[17] The longitudinal factor in Eq. (11) results from the dependencies: beam height $\sim \sqrt{\beta_y(s)}$, tune shift $\sim \beta_y(s) \times$ charge density, $\beta_y(s)/\beta_y(0) = 1 + (s/\beta_y(0))^2$. A strictly faithfull treatment would convolve the square root factor in Eq. (11) with the longitudinal density distribution, but this has not been done.

[18] In the jargon of ordinary differential equations introducing the Fourier series of Eq. (12) converts a "Mathieu equation" into a "Hill equation".[6]

[19] The stability limits (24) (though not the growth rate in the interior) could have been determined by setting $\dot{a} = \dot{b} = 0$ in Eq. (21). The justification is that the amplitude neither grows nor shrinks at the ends of the stop band.

[20] The effect of dependence of μ_s on a_s has not been investigated.

[21] For same-sign colliders $\xi < 0$ and the negative-Q_x side is the "good side" of resonances. This has been confirmed numerically.

[22] It is the equality of cosines, rather than the equality of tunes, that causes resonance. To handle this all tunes can be aliased into fractional tunes in a range from 0 to 0.5. This effectively reduces the resonance-free fractional tune landscape by a factor of 2.

[23] Note the distincion between the symbol ε for frequency deviations and the symbol ϵ for Courant-Snyder invariants.

[24] Unless otherwise noted, summations over m run over all integers from $-\infty$ to ∞.

[25] Ordinarily an *ansatz* like Eq. (B2) would be made in preparation for finding nonlinear harmonics, intending to truncate higher Fourier terms. Here, because the drive is parametric, the equations will remain linear. There will be a certain amount of "leakage" if the series is truncated, but this is mainly a question of convenience, and there is no possibility of the chaotic motion that characterizes

nonlinear equations. This may be somewhat academic as the growth the equations exhibit can lead to amplitudes for which nonlinearity becomes important and the linearity assumption loses validity.

[26] Though the synchrotron and horizontal oscillation frequencies are certain to be incommensurate in practice, without care they are likely to be commensurate in a simulation in which both values are "put in by hand". This could lead to unphysical resonant artifacts.

[27] For a parametrically-driven mechanical system, described by a non-autonomous differential equation such as the Mathieu equation or the Hill equation, Eqs. (B12) would be known as "Hill equations".

[28] For convenience in all subsequent formulas we set $\pi B_n = 1$. This is equivalent to having redefined ξ, so the factors can be restored by the replacement $\xi \to \pi B_n \xi$. As it happens 1 *is* a typical value for πB_n.